Dear Dr. Eliza Harris,

We appreciate the valuable suggestions given by the reviewers for improving the quality of our manuscript. In this document, we describe how we addressed their comments. Detailed responses to each comment are given below (in blue). We have addressed all the comments, and incorporated the comments or suggestions in the revised manuscript. Thank you very much for your consideration.

Sincerely,

Lei Liu

On behalf of all co-authors

## Response to Referee #1

Received and published: 17 Apr 2020

This study reviews recent literatures on estimating reactive nitrogen (Nr) deposition using the satellite retrievals of NO2 and NH3, proposes a framework of using satellite data to estimate Nr deposition, and suggests a few research challenges. The topic of nitrogen deposition is important, and the compilation of recent literatures on reactive nitrogen deposition is useful to the research community. However, the manuscript mainly gives general descriptions of the previous results but lacks critical analysis and synthesis. The uncertainties in satellite measurements and chemical transport models, which are key to estimating Nr deposition based on satellite column measurements, are not addressed in detail. Overall, the scientific values of this work could be enhanced by more in-depth discussion of the advancement, challenges, and directions for future research.

The authors appreciate the valuable suggestions given by Referee #1 for improving the overall quality of the manuscript. In this document, we describe how we addressed the reviewer's comments. Detailed responses to each comment are given below (in blue).

**Specific comments:**

1. The authors highlight the advantages of satellite-based method compared to

ground-based monitoring and ACTM simulation method. But there are significant uncertainties of satellite column measurements, especially for $NH_3$. In addition, the satellite-based method strongly depends on the ACTM simulation. What are the key uncertainties of the ACTM related to deposition estimates? How do the uncertainties in satellite measurements and ACTM affect satellite-based estimation? What are recommendations to reduce these uncertainties?

Yes, the uncertainties mainly came from the satellite retrievals and ACTM simulation. We did not aim to improve the accuracy of the satellite observations or the ACTM themselves, but to combine their advantages to gain surface $N_r$ concentrations with better performance with the ground-based measurements. We have added the following text for more clarifications in the discussion:

"For the dry deposition, the uncertainty mainly came from the satellite-derived estimates using the modeled vertical profiles. The uncertainty of vertical profiles modeled by CTM mainly resulted from the chemical and transport mechanisms. We recommend using the Gaussian function to determine the height of surface $NO_2$ and $NH_3$ concentrations that best matched with the ground-based measurements. There may exist systematic biases by simply using the relationship of $NO_2$ columns and surface concentration to estimate satellite surface $NO_2$ concentrations."

2. The authors propose a framework for combining satellite data, ground-based monitoring and ACTM (Figure 1). But it is not clear if it is a new idea. It seems that the approach has already been used in previous studies as indicated in the literatures shown in sections after Figure 1.

Yes, it's a new framework proposed in this study. Previous studies mainly focused on the methods to estimate surface $NO_2$ concentrations, while **Fig. 1** shows the general approach for estimating all $N_r$ spices on both concentration and deposition.

3. The title contains “Nr concentration and deposition”, but the introduction part and the framework only mention “deposition”. In my opinion, the estimation of Nr concentrations is just a part of the estimation of Nr depositions. There are many other studies which have offered more in-depth discussions of column concentrations of NO2 and NH3. I am not saying that concentrations cannot be shown but suggest framing the paper with a clearer focus on deposition.

Thanks for your suggestion. But, we think the introduction is appropriate since the estimation of $N_r$ concentrations is just a part of the estimation of dry $N_r$ depositions. The title included both the “$N_r$ concentration” and “deposition” because we reviewed on the methods of estimating both surface $N_r$ concentration and $N_r$ deposition.

4. Line 193-195: Why may this method lead to an underestimation of surface NO2 concentration? In your proposed framework, the similar method has been used to estimate the surface NO2 concentration. Why is there no large underestimation in your validation? While you use the Gaussian function to fit the vertical concentration profile, but for the surface layer, you still use the ACTM derived the relationship between the NO2 column and surface NO2 concentration.

No, the methods in this study were different from the previous studies. We did not simply use the relationship between the $NO_2$ column and surface $NO_2$ concentration from the CTM. As presented in the main text, we can estimate surface $NO_2$ concentration at any height by using the Gaussian function. We used the surface $NO_2$ concentration at a certain height which best matched with the ground-based measurements.

5. Line 405-409: The derived NO2 columns from these satellites are quite different. Can you give some suggestions to the readers about which satellite data to use? Why do you choose OMI NO2 in your estimation? What are the results if you use other

satellite data?

The readers can use any satellite data combining the Gaussian function to estimate surface $NO_2$ concentrations. They can use surface $NO_2$ concentrations at a certain height which best matched with the ground-based measurements. The key is not selecting which satellite data we should use, but determining which height of surface $NO_2$ concentrations that better matched with the ground-based measurements by Gaussian function.

6. Line 550-552: Can the similar method in equation 9 and 10 be used to estimate wet reduced Nr depositions? What are the different challenges for the estimations of wet reduced Nr depositions, compared with oxidized Nr?

Yes, the methods were the same for estimating both oxidized and reduced $N_r$ deposition. We did not identify big difference in the estimations of wet oxidized and reduced $N_r$ depositions.

7. Section 5: For the trend estimation of Nr concentrations and depositions, have you conducted ACTM simulation for each year? The changes in emission and meteorology can significantly affect the Nr vertical profile and Nr species ratio, which are important in your satellite-based estimation.

Yes, we did. Please note that the simulated profile function has a general rule, which can be well simulated by Gaussian function for any year (for our case during 2005-2016). Thus, there is no need to simulate the vertical profile of $NO_2$ and $NH_3$ for each year.

8. Line 567-569: This statement needs to be modified. As mentioned above, the satellite-based method strongly depends on the ACTM simulation. The uncertainties in emission inventories and other parts of ACTM can also significantly affect the vertical distribution of pollutants and the ratios of NO2 and other Nr species (e.g.

HNO3, NH4+).

No, the emission inventories should not affect the vertical profiles shapes using Gaussian function, but the transport and chemical mechanism in the CTM may affect the accuracy of the vertical profile distribution. We mean that the satellite-based methods did not need to rely on the accuracy of the statistical emission data.

9. Line 697: Are there any previous studies using a mechanism method to estimate Nr deposition?

As far as we know, previous studies using satellite $NO_2$ and $NH_3$ column to estimate wet $N_r$ deposition were through a statistical way, and no studies were done from a mechanism perspective.

**Minor comments:**

1. The authors should give the definition of reactive nitrogen (Nr). "Nr (such as NO3- and NH4+)" is mentioned in line 48, and "Nr (NOx and NH3)" is mentioned in line 59. This is confusing.

We have added the following text for clarifications:

"$N_r$ refers to the general term of N-containing substances in atmosphere, plants, soils and fertilizers that are not combined with carbon".

2. Line 57, change "mineral energy" to "fossil energy".

We have revised it as suggested.

3. Line 83, add "and" between the two words "accurate quantitative".

We have revised it as suggested.

4. Line 145-146: "Tian et al." should be "Tan et al. (2018)".

We have revised it as suggested.

5. Line 170: "Cheng et al. (Cheng et al., 2013)" should be "Cheng et al. (2013)". Please check the citation format throughout the manuscript.

We have checked the citation format throughout the manuscript as suggested.

6. Line 170-171: This sentence is not easy to understand. Please revise it.

We have revised it as follows:

"This method used the simple linear model and did not consider the vertical profiles of $NO_2$ (Cheng et al., 2013)"

7. Line 198-200: The study of Larkin et al., 2017 should be put in the previous paragraph discussing the method using the satellite data and statistical model. I think that the authors are discussing the method using the satellite data and ACTM-derived relationship in this paragraph.

No, Larkin et al. (2017) were also based on the satellite data and ACTM-derived relationship similar to Geddes et al. (2016), and it should be there.

8. Line 225-232: This information based on Jia et al. (2016) has been mentioned in line 176-184. They are repetitive.

We have removed it to avoid repetitive.

**Response to Referee #2**

Received and published: 1 June 2020

We thank the reviewer very much for the detailed and valuable comments. We believe that addressing the issues raised by the reviewer will considerably improve the quality of our manuscript. Please see our response to each comment below (in blue).

This manuscript presents an overview of Global Estimates of Surface Reactive Nitrogen Concentration and Deposition Using Satellite Observation. The authors discuss recent advances of estimating surface Nr concentration and deposition, present a framework of using satellite data to estimate surface Nr concentration and deposition, and summarize the existing challenges for estimating surface Nr

concentration and deposition using the satellite-based methods.

The manuscript is clearly written and logically organized. It provides sufficient and up-to-date literature citations. Listed below comments and suggestions for changes are relatively minor, but should be carefully considered. I recommend publication after addressing following comments:

1. L290: It is unclear to me how the vertical resolution of GEOS-Chem can resolve the vertical gradients that are likely to exist in source regions. The authors should clarify these several issues: (1) the vertical structure of the model, (2) the measurement characteristics of the surface observation (including height), (3) how this information is used to calculate surface concentrations.

IASI $NH_3$ retrievals are column data that has no vertical profile information. We gained surface $NH_3$ concentration by using modeled $NH_3$ vertical profiles from GEOS-Chem including 47 layers. We constructed the Gaussian model to fit the 47 layers' vertical $NH_3$ concentrations, which can generate the continuous $NH_3$ profile. Hence, based on the constructed the Gaussian model, we can obtain satellite-based $NH_3$ concentration at any height. More importantly, the constructed the Gaussian model has general rules, appropriate for converting satellite columns to surface concentration simply. Please refer to the Sect. 3.1 for more details.

2. Fig. 10b: It is true that NH3 can be more accurately retrieved in one region than another depending on the thermal contrast. But it is not clear to me why this would be so much better in China than that in the US? I guess it is also just a matter of detection limits? It could also be related to more reliable simulation of mixing, depending on sufficient observational input into the parent weather model. Please clarify this issue.

We agree with you that the accuracy of IASI-retrieved surface $NH_3$ concentrations in different regions is highly linked with the thermal contrast (TC) and the simulation of

$NH_3$ mixing from GEOS-Chem. The accuracy for satellite estimates over different area is related to the thermal contrast. The lowest uncertainties occurred when high columns and high TC coincide. In case either of them decreases, the uncertainty will gradually increase. In case both the TC and column are low, all sensitivity to $NH_3$ is lost. When high TC and high $NH_3$ columns (high HRI) occurs, the major contribution to the uncertainty results from the thickness of the $NH_3$ layer, the surface temperature as well as the temperature profile (Whitburn et al., 2016). We have added following text for clarification in the Sect. 4.2: "Higher correlation over China than other regions for the satellite estimates is linked to the detection limits by the instruments and thermal contrast (Liu et al., 2019).".

3. L531: For the estimated ammonia deposition, its uncertainties from remote sensing and models should be discussed more in this manuscript.

We have added the following text for further describing the uncertainties in the Sect. 4.2:

"The satellite $NH_3$ retrievals were affected by the detection limits of the satellite instruments and thermal contrast. Higher accuracy could be gained with higher thermal contrast and $NH_3$ abundance. Instead, the uncertainties of $NH_3$ retrievals would be higher with lower thermal contrast and $NH_3$ abundance."

4. title: I suggest to change the satellite observation to "satellite retrievals" since IASI NH3 data were not a direct satellite observation but a reanalysis data using the statistical methods.

We have revised it as suggested.

5. L30: The abbreviation must be defined for the first occurrence.

We have removed these abbreviations.

6. L137: Replace ACTM with Atmospheric chemistry transport model

We have revised it as suggested.

7. L306: Added the references of the equations.

We have added the reference as suggested.

8. L333: Added the references of the equations.

We have added the reference as suggested.

# Reviewing Global Estimates of Surface Reactive Nitrogen Concentration and Deposition Using Satellite Retrievals

Lei Liu [a, *], Xiuying Zhang [b], Wen Xu [c], Xuejun Liu [c], Xuehe Lu [b], Jing Wei [d, e], Yi Li [f], Yuyu Yang [a], Zhen Wang [b], Anthony Y. H. Wong [g]

[a] College of Earth and Environmental Sciences, Lanzhou University, Lanzhou 730000, China

[b] International Institute for Earth System Science, Nanjing University, Nanjing, 210023, China

[c] College of Resources and Environmental Sciences, National Academy of Agriculture Green Development, China Agricultural University, Beijing, 100193, China

[d] State Key Laboratory of Remote Sensing Science, College of Global Change and Earth System Science, Beijing Normal University, Beijing, China

[e] Department of Atmospheric and Oceanic Science, Earth System Science Interdisciplinary Center, University of Maryland, College Park, MD, USA

[f] Chief Technology Officer SailBri Cooper Inc., Beaverton OR, 97008, USA

[g] Department of Earth and Environment, Boston University, Boston, MA 02215, USA

* Correspondence to Lei Liu (liuleigeo@lzu.edu.cn).

## Abstract

Since the industrial revolution, human activities have dramatically changed the nitrogen (N) cycle in natural systems. Anthropogenic emissions of reactive nitrogen ($N_r$) can return to the earth's surface through atmospheric $N_r$ deposition. Increased $N_r$ deposition may improve ecosystem productivity. However, excessive $N_r$ deposition can cause a series of negative effects on ecosystem health, biodiversity, soil, and water. Thus, accurate estimations of $N_r$ deposition are necessary for evaluating its

environmental impacts. The United States, Canada and Europe have successively launched a number of satellites with sensors that allow retrieval of atmospheric $NO_2$ and $NH_3$ column density, and therefore estimation of surface $N_r$ concentration and deposition at an unprecedented spatiotemporal scale. Atmosphere $NH_3$ column can be retrieved from atmospheric infra-red emission, while atmospheric $NO_2$ column can be retrieved from reflected solar radiation. In recent years, scientists attempted to estimate surface $N_r$ concentration and deposition using satellite retrieval of atmospheric $NO_2$ and $NH_3$ columns. In this study, we give a thorough review on recent advances of estimating surface $N_r$ concentration and deposition using the satellite retrievals of $NO_2$ and $NH_3$, present a framework of using satellite data to estimate surface $N_r$ concentration and deposition based on recent works, and summarize the existing challenges for estimating surface $N_r$ concentration and deposition using the satellite-based methods. We believe that exploiting satellite data to estimate $N_r$ deposition has a broad and promising prospect.

**Keywords**

Nitrogen deposition; Satellite retrieval; Surface concentration; Oxidized and reduced $N_r$

## 1. Introduction

Nitrogen (N) exists in three forms in the environment including reactive nitrogen ($N_r$), organic nitrogen (ON) and nitrogen gas ($N_2$) (Canfield et al., 2010). $N_2$ is the main component of air, accounting for 78% of the total volume of air, but it cannot be directly used by most plants. $N_r$ refers to the general term of N-containing substances in atmosphere, plants, soils and fertilizers that are not combined with carbon. $N_r$ (such as $NO_3^-$ and $NH_4^+$) is the main form of N that can be directly used by most plants, but the content of $N_r$ in nature is much lower compared with ON and $N_2$ (Vitousek et al.,

1997;Nicolas and Galloway, 2008). The supply of $N_r$ is essential for all life forms and contributes to the increase in agricultural production, thus providing sufficient food for the growing global population (Galloway et al., 2008;David et al., 2013;Galloway et al., 2004b;Erisman et al., 2008). Before the industrial revolution, $N_r$ mainly came from natural sources such as biological N fixation, lightning and volcanic eruption (Galloway et al., 2004a). Since the industrial revolution, human activities (e.g. agricultural development, combustion of fossil energy) have greatly perturbed the N cycle in natural systems (Canfield et al., 2010;Kim et al., 2014;Lamarque et al., 2005).

$N_r$ ($NO_x$ and $NH_3$) emitted to the atmosphere will return to the earth surface through atmospheric deposition (Liu et al., 2011). Atmospheric $N_r$ deposition refers to the process in which $N_r$ are removed from the atmosphere, including wet (rain and snow) and dry (gravitational settling, atmospheric turbulence, etc.) deposition (Xu et al., 2015;Zhang et al., 2012;Pan et al., 2012). The input of $N_r$ over terrestrial natural ecosystems primarily comes from the $N_r$ deposition (Shen et al., 2013;Sutton et al., 2001;Larssen et al., 2011). In the short term, atmospheric $N_r$ deposition can increase the $N_r$ input to ecosystems, which promotes plant growth and enhances ecosystem productivity (Erisman et al., 2008;Sutton et al., 2013). However, excessive atmospheric $N_r$ deposition also causes a series of environmental problems (Liu et al., 2017d). Due to the low efficiency of agricultural N application, plenty of $N_r$ is lost through runoff, leaching and volatilization, causing serious environmental pollution. Excessive $N_r$ deposition may aggravate the plant's susceptibility to drought or frost, reduce the resistance of plant to pathogens or pests, and further affect the physiology and biomass distribution of vegetation (ratio of roots, stems and leaves) (Stevens et al., 2004;Nadelhoffer et al., 1999;Bobbink et al., 2010;Janssens et al., 2010). Excessive

$N_r$ leads to eutrophication and related algal blooms over aquatic ecosystems, reducing water biodiversity (Paerl et al., 2014), while excessive $N_r$ in drinking water also poses a threat to human health (Zhao et al., 2013). Therefore, monitoring and estimation of surface $N_r$ concentration and deposition on the global scale are of great importance and urgency.

The methods of estimating atmospheric $N_r$ deposition can be divided into three categories: ground-based monitoring, atmospheric chemical transport modeling (ACTM) and satellite-based estimation. Ground-based monitoring is considered to be the most accurate and quantitative method, which can effectively reflect the $N_r$ deposition in local areas. ACTM can simulate the processes of $N_r$ chemical reaction, transport, and deposition, as well as the vertical distribution of $N_r$. Satellite-based estimation establishes empirical, physical or semi-empirical models by connecting the ground-based $N_r$ concentrations and deposition with satellite-derived $N_r$ concentration. This study focuses on reviewing the recent development of satellite-based methods to estimate $N_r$ deposition. We firstly give a brief introduction to the progress of ground-based monitoring, ACTM-based methods, and then present a detailed framework of using satellite observation to estimate dry and wet $N_r$ deposition (including both oxidized and reduced $N_r$). Next, we review the recent advances of the satellite-based methods of estimating $N_r$ deposition. Finally, we discuss the remaining challenges for estimating surface $N_r$ concentration and deposition using satellite observation.

## 2 Methods for Estimating Surface $N_r$ Concentration and Deposition

### 2.1 Ground-based Monitoring

Ground-based monitoring of $N_r$ deposition can be divided into two parts: wet and dry $N_r$ deposition monitoring. Since the 1970s, there have been large-scale monitoring

networks focusing on the wet $N_r$ deposition. The main large-scale regional monitoring networks include Canadian Air and Precipitation Monitoring Network (CAPMoN), Acid Deposition Monitoring Network in East Asia (EANET), European Monitoring and Evaluation Program (EMEP), United States National Atmospheric Deposition Program (NADP), World Meteorological Organization Global Atmosphere Watch Precipitation Chemistry Program, and Nationwide Nitrogen Deposition Monitoring Network in China (NNDMN) (Tan et al., 2018;Vet et al., 2014). The detailed scientific objectives of the wet $N_r$ deposition observation networks vary, but most of the observation networks mainly concentrate on the spatiotemporal variation of wet deposition of ions including $N_r$ compounds, the long-term trends of ions in precipitation, and the evaluation of ACTMs.

Compared with wet $N_r$ deposition monitoring, dry $N_r$ deposition monitoring started late, due to the limitation of monitoring technology since it is more difficult to be quantified (affected greatly by surface roughness, air humidity, climate and other environmental factors) (Liu et al., 2017c). Dry $N_r$ deposition observation networks include US ammonia monitoring network (AMoN), CAPMoN, EANET and EMEP. The monitoring methods of dry $N_r$ deposition are mainly divided into direct monitoring (such as dynamic chambers) and indirect monitoring (such as inferential methods). The inferential model is widely applied in ground-based monitoring networks (such as EANET and NNDMN), mainly because this method is more practical and simpler. In inferential models, dry deposition is divided into two parts: surface $N_r$ concentrations and the deposition velocity ($V_d$) of $N_r$ (Nowlan et al., 2014). $V_d$ can be estimated by meteorology, land use types of underlying surface as well as the characteristics of each $N_r$ component itself using resistance models (Nemitz et al., 2001). Thus, dry $N_r$ deposition monitoring networks only need to focus on the

126 quantification of surface concentration of individual $N_r$ components. The $N_r$
127 components in the atmosphere are very complex, including $N_2O_5$, HONO, $NH_3$, $NO_2$,
128 $HNO_3$ and particulate $NH_4^+$ and $NO_3^-$. Most monitoring networks include the major
129 $N_r$ species such as gaseous $NH_3$, $NO_2$, $HNO_3$ and the particles of $NH_4^+$ and $NO_3^-$.
130 Effort of ground-based $N_r$ deposition monitoring mostly concentrates on wet $N_r$
131 deposition, while observations of dry $N_r$ deposition are relatively scarce especially for
132 surface $HNO_3$ and $NH_4^+$ and $NO_3^-$. Second, most observation networks focus on a few
133 years or a certain period of time, leading to the lack of long-term continuously
134 monitoring on both wet and dry $N_r$ deposition. More importantly, the global $N_r$
135 deposition monitoring network has not been established, and the sampling standards
136 in different regions are not unified. These outline the potential room for improvement
137 of ground-based $N_r$ deposition monitoring.

138 **2.2 Atmospheric Chemistry Transport Model (ACTM) Simulation**

139 An ACTM can simulate $N_r$ deposition at regional or global scales through explicitly
140 representing the physical and chemical processes of atmospheric $N_r$ components
141 (Zhao et al., 2017;Zhang et al., 2012). Wet $N_r$ deposition flux is parameterized as
142 in-cloud, under-cloud and precipitation scavenging (Amos et al., 2012;Levine and
143 Schwartz, 1982;Liu et al., 2001;Mari et al., 2000), while dry deposition flux can be
144 obtained as the product of surface $N_r$ concentration and $V_d$, which is typically
145 parameterized as a network of resistances (Wesely and Hicks, 1977). Based on the
146 integrated results of 11 models of HTAP (hemispheric transport of air pollution), Tan
147 et al. found that about 76%-83% of the ACTM's simulation results were ±50% of the
148 monitoring values, and the modeling results underestimated the wet deposition of
149 $NH_4^+$ and $NO_3^-$ over Europe and East Asia, and overestimated the wet deposition of
150 $NO_3^-$ over the eastern US (Tan et al., 2018). Though regional ACTMs can be

151 configured at very high horizontal resolution (e.g., 1 ×1 $km^2$) (Kuik et al., 2016), the
152 horizontal resolution of global ACTMs are relatively coarse (1 °×1 °-5 °×4 °) (Williams
153 et al., 2017), which cannot indicate the local pattern of $N_r$ deposition. On the other
154 hand, the $N_r$ emission inventory used to drive an ACTM is highly uncertain, with the
155 uncertainty of the $NO_x$ emission at about ±30-40%, and that of $NH_3$ emission at about
156 ±30-80% (Zhang et al., 2009;Cao et al., 2011).

157 **2.3 Satellite-based Estimation of Surface $N_r$ Concentration and Deposition**

158 Satellite observation has wide spatial coverages and high resolution, and is
159 spatiotemporally continuous. Atmospheric $NO_2$ and $NH_3$ columns can be derived
160 from satellite measurements with relatively high accuracy (Van Damme et al.,
161 2014a;Boersma et al., 2011), providing a new perspective about atmospheric $N_r$
162 abundance.

163 Satellite instruments that can monitor $NO_2$ in the atmosphere include GOME (Global
164 Ozone Monitoring Experience), SCIAMACHY (SCanning Imaging Absorption
165 SpectroMeter for Atmospheric ChartographY), OMI (Ozone Monitoring Instrument),
166 GOME-2 (Global Ozone Monitoring Experience-2). Some scholars applied satellite
167 $NO_2$ columns to estimate the surface $NO_2$ concentration, and then dry $NO_2$ deposition
168 by combining the surface $NO_2$ concentration and modeled $V_d$. Cheng et al. established
169 a statistical model to estimate the surface $NO_2$ concentration based on the
170 SCIAMACHY $NO_2$ columns, and then estimated the dry deposition of $NO_2$ over
171 eastern China (Cheng et al., 2013). This method used the simple linear model and did
172 not consider the vertical profiles of $NO_2$ (Cheng et al., 2013). Lu et al. established a
173 multivariate linear regression model based on the SCIAMACHY and GOME $NO_2$
174 columns, meteorological data and ground-based monitoring $N_r$ deposition, and then
175 estimated the global total $N_r$ deposition (Lu et al., 2013). Lu et al. could not

distinguish the contribution of dry and wet $N_r$ deposition using the multivariate linear regression model (Lu et al., 2013). Jia et al. established a simple linear regression model based on OMI tropospheric $NO_2$ column and ground-based surface $N_r$ concentration, and then estimated the total amounts of dry $N_r$ deposition (Jia et al., 2016). Jia et al. used OMI tropospheric $NO_2$ column to estimate the dry deposition of reduced $N_r$ deposition ($NH_3$ and $NH_4^+$), which could also bring great errors since the OMI $NO_2$ column could not indicate the $NH_3$ emission. These studies highlight the problem of using only $NO_2$ columns to derive total $N_r$ deposition, that $NO_2$ columns give us highly limited information about the abundance of reduced $N_r$ ($NH_3$ and $NH_4^+$).

Lamsal et al. first used the relationship between the $NO_2$ column and surface $NO_2$ concentration at the bottom layer simulated by an ACTM to convert OMI $NO_2$ column to surface $NO_2$ concentration (Lamsal et al., 2008). A series of works (Lamsal et al., 2013;Nowlan et al., 2014;Kharol et al., 2018) have effectively estimated regional and global surface $NO_2$ concentration using satellite $NO_2$ column combining with ACTM-derived relationship between the $NO_2$ column and surface $NO_2$ concentration simulated. It is worth mentioning that Nowlan et al. applied OMI $NO_2$ column to obtain the global dry $NO_2$ deposition during 2005-2007 for the first time (Nowlan et al., 2014). However, using satellite $NO_2$ column and ACTM-derived relationship between the $NO_2$ column and surface $NO_2$ concentration may lead to an underestimation of surface $NO_2$ concentration. Kharol et al. found that the satellite-derived surface $NO_2$ concentration using the above method is only half of the observed values (Kharol et al., 2015). To resolve such potential underestimation, Larkin et al. established a statistical relationship between the satellite-derived and ground measured surface $NO_2$ concentration, and then calibrated the satellite-derived

surface $NO_2$ concentration using the established relationship (Larkin et al., 2017).

Some researchers also estimated other $N_r$ components (such as particulate $NO_3^-$) based on satellite $NO_2$ column. Based on the linear model between $NO_2$, $NO_3^-$, $HNO_3$ obtained by ground-based measurements, Jia et al. calculated the surface $NO_3^-$ and $HNO_3$ concentration using satellite-derived surface $NO_2$ concentration and their relationship (Jia et al., 2016). Geddes et al. reconstructed the $NO_x$ emission data by using the satellite $NO_2$ column, and then estimated the global $NO_x$ deposition by an ACTM, but the spatial resolution of global $NO_x$ deposition remains low (2 °×2.5 °), failing to exploit the higher resolution of satellite observation (Geddes and Martin, 2017).

Comparing with $NO_2$, the development of satellite $NH_3$ monitoring is relatively late. Atmospheric $NH_3$ was first detected by the TES in Beijing and Los Angeles (Beer et al., 2008). The IASI sensor also detected atmospheric $NH_3$ from a biomass burning event in Greece (Coheur et al., 2009). Subsequently, many scholars began to develop more reliable satellite $NH_3$ column retrievals (Whitburn et al., 2016;Van Damme et al., 2014a), validate the satellite-retrieved $NH_3$ column with the ground-based observation (Van Damme et al., 2014a;Dammers et al., 2016;Li et al., 2017), and compare the satellite $NH_3$ column with the aircraft measured $NH_3$ column (Van Damme et al., 2014b;Whitburn et al., 2016). In recent years, some scholars have carried out the works of estimating surface $NH_3$ concentration based on satellite $NH_3$ column. Liu et al. obtained the satellite-derived surface $NH_3$ concentration in China based on the IASI $NH_3$ column coupled with an ACTM, and deepened the understanding of the spatial pattern of surface $NH_3$ concentration in China (Liu et al., 2017b). Similarly, Graaf et al. carried out the relevant work in Europe based on the IASI $NH_3$ column coupled with an ACTM, and estimated the dry $NH_3$ deposition in West Europe (Van

der Graaf et al., 2018). Jia et al. first constructed the linear model between surface $NO_2$ and $NH_4^+$ concentration based on ground monitoring data, and then calculated the $NH_4^+$ concentration using satellite-derived surface $NO_2$ concentration and their relationship (Jia et al., 2016). However, as the emission sources of $NO_x$ (mainly from transportation and energy sectors) and $NH_3$ (mainly from agricultural sector) are different (Hoesly et al., 2018), the linear model between surface $NO_2$ and $NH_4^+$ concentration may lead to large uncertainties in estimating the global $NH_4^+$ concentration. There is still no report about the satellite-derived dry and wet reduced $N_r$ deposition using satellite $NH_3$ column at a global scale. As reduced $N_r$ plays an important role in total $N_r$ deposition, satellite $NH_3$ should be better utilized to help estimate reduced $N_r$ deposition.

### 2.4 Problems in Estimating Global $N_r$ Deposition

The spatial coverage of ground monitoring sites focusing on $N_r$ deposition is still not adequate, and the monitoring standards and specifications in different regions of the world are not consistent, presenting a barrier to integrating different regional monitoring data. Large uncertainties exist in $N_r$ emission inventory used to drive the ACTMs, and the spatial resolution of the modeled $N_r$ deposition by ACTMs is coarse. Using satellite monitoring data to estimate surface $N_r$ concentration and deposition is still in its infancy, especially for reduced $N_r$.

Some scholars tried to use satellite $NO_2$ and $NH_3$ column to estimate the surface $N_r$ concentration and dry $N_r$ deposition. However, there are relatively few studies on estimating wet $N_r$ deposition. In addition, the development of satellite monitoring for $NH_3$ in the atmosphere is relatively late (compared with $NO_2$). At present, IASI $NH_3$ data have been widely used, while the effective measurements of TES are less than IASI; CrIS and AIRS $NH_3$ column products are still under development. There are

three main concerns in high-resolution estimation of surface $N_r$ concentration and deposition based on satellite $N_r$ observation. (1) How to effectively couple the satellite high-resolution $NO_2$ and $NH_3$ column data with the vertical profiles simulated by an ACTM, and then estimates the surface $N_r$ concentrations? This step is the key to simulate the dry $N_r$ deposition. (2) How to construct a model for estimating dry $N_r$ deposition including all major $N_r$ species based on satellite $NO_2$ and $NH_3$ column, and then estimates the dry $N_r$ deposition at a high spatial resolution? (3) How to combine the high-resolution satellite $NO_2$ and $NH_3$ column data and ground-based monitoring data to construct wet $N_r$ deposition models, and then estimate the wet $N_r$ deposition at a high spatial resolution?

## 3. Framework of Estimating Surface $N_r$ Concentration and Deposition Using Satellite Observation

We give a framework of using satellite observation to estimate surface $N_r$ concentration and deposition as shown in **Fig. 1** based on recent advances.

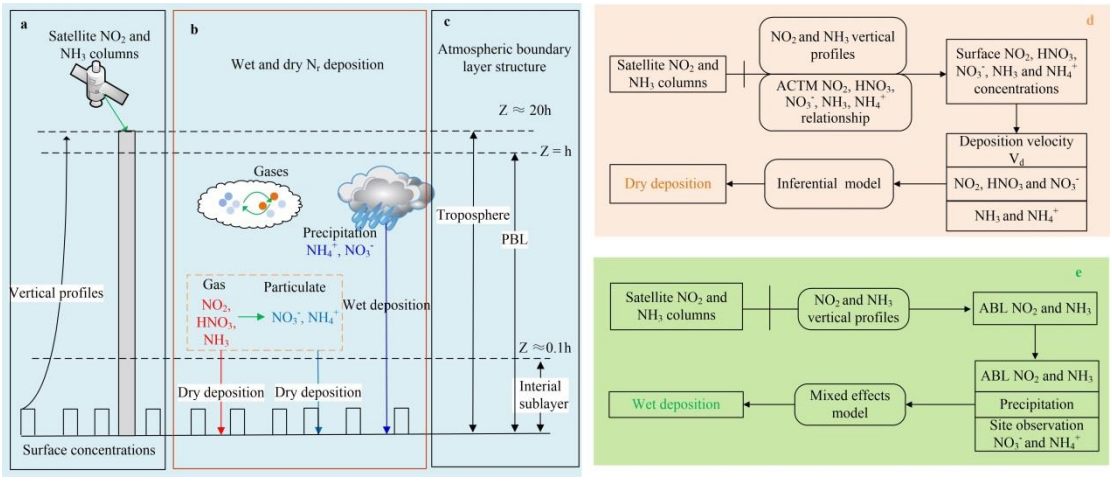


**Fig. 1 Schematic diagram of dry and wet $N_r$ deposition.** (a) indicates satellite observed $NO_2$ and $NH_3$ column, and the vertical profiles by an ACTM; (b) shows dry and wet $N_r$ deposition including the major $N_r$ species (gaseous $NO_2$, $HNO_3$, $NH_3$, particulate $NO_3^-$ and $NH_4^+$, as well as wet $NO_3^-$ and $NH_4^+$ in precipitation); (c) illustrates atmospheric vertical structures including the troposphere (satellite observation), atmospheric boundary layer (ABL), interfacial sub-layer; (d) and (e) represent procedures of calculating the dry and wet $N_r$ deposition.

### 3.1 Conversion of Satellite $NO_2$ and $NH_3$ Column to Surface $N_r$ Concentration

An ACTM can simulate the vertical profiles of $NO_2$ and $NH_3$ with multiple layers from the surface to the troposphere. For example, the GEOS-Chem ACTM includes 47 vertical layers from the earth surface to the top of the stratosphere. Most previous studies estimated the ratio of surface $N_r$ concentration (at the first layer) to total columns by an ACTM, and then multiply the ratio by satellite columns to estimate satellite-derived surface concentration (Geddes et al., 2016;Graaf et al., 2018;Nowlan et al., 2014).

Another approach tries to fit general vertical profiles of $NO_2$ and $NH_3$ (Zhang et al., 2017;Liu et al., 2017b;Liu et al., 2017c), and then estimate the ratio of $N_r$ concentration at any height to total $N_r$ columns, and finally multiply the ratio by satellite $NO_2$ and $NH_3$ columns. This approach has an advantage compared with the previous one for that $NO_2$ and $NH_3$ concentration at all altitude included in ACTM simulations can be estimated.

Taking the estimation of surface $NO_2$ concentration using the latter approach as an example, the methods and steps are introduced in the following.

Step 1: Calculate the monthly mean $NO_2$ concentrations at all layers simulated by an ACTM.

Step 2: Construct the vertical profile function of $NO_2$. Multiple Gaussian functions are used to fit the vertical distribution of $NO_2$ based on the monthly $NO_2$ concentrations at all layers calculated in Step 1, in which the independent variable is the height (altitude), and the dependent variable is $NO_2$ concentration at a certain height.

The basic form of single Gaussian function is (Zhang et al., 2017;Liu et al., 2017b;Liu et al., 2017c;Whitburn et al., 2016):

$$\rho = \rho_{max} e^{-(\frac{z-z_0}{\sigma})^2} \quad (1)$$

where Z is the height of a layer in the ACTM; $\rho_{max}$, $Z_o$ and σ are the maximum $NO_2$ concentration, the corresponding height with the maximum $NO_2$ concentration and the thickness of $NO_2$ concentration layer (one standard error of Gaussian function).

There are two basic forms of profile shapes of $NO_2$: (1) $NO_2$ concentration reaches the maximum concentration when reaching a certain height ($Z_o \neq 0$). As the height increases, the $NO_2$ concentration begins to decline; (2) $NO_2$ concentration is basically concentrated on the earth surface ($Z_o=0$). These two cases are the ideal state of the vertical distribution of $NO_2$ concentration. In reality, single Gaussian fitting may not capture the vertical distribution of $NO_2$ well. To improve the accuracy of fitting, the sum of multiple Gaussian functions can be used (Liu et al., 2019):

$$\rho(Z) = \sum_{i=1}^{n} \rho_{max,i} e^{-(\frac{Z-Z_{0,i}}{\sigma_i})^2} \quad (2)$$

Step 3: Calculate the ratio of $NO_2$ concentration at the height of $h_G$ to total columns ($\int_0^{h_{trop}} \rho(Z)\,dx$), and then multiply the ratio by satellite column ($S_{trop}$). The satellite-derived $N_r$ concentration at the height of $h_G$ can be calculated as:

$$S_{G\_NO2} = S_{trop} \times \frac{\rho(h_G)}{\int_0^{h_{trop}} \rho(Z)dx} \quad (3)$$

Step 4: Convert the instantaneous satellite-derived surface $NO_2$ concentration ($S_{G\_NO2}$) to daily average ($S_{G\_NO2}*$) using the ratio of average surface $NO_2$ concentration ($G_{ACTM}^{1-24}$) to that at satellite overpass time ($G_{ACTM}^{overpass}$) by an ACTM (Liu et al., 2020):

$$S_{G\_NO2}* = \frac{G_{ACTM}^{1-24}}{G_{ACTM}^{overpass}} \times S_{G\_NO2} \quad (4)$$

The method for estimating the surface $NH_3$ concentration ($S_{G\_NH3}*$) is similar to that for estimating the surface $NO_2$ concentration.

### 3.2 Estimating Surface Concentration of Other $N_r$ Species

At present, only $NO_2$ and $NH_3$ column can be retrieved reliably, and there are no

reliable satellite retrievals of $HNO_3$, $NH_4^+$ and $NO_3^-$. For example, the IASI $HNO_3$ product is still in the stage of data development and verification (Ronsmans et al., 2016). Previous studies firstly derive the relationship between $N_r$ species by an ACTM or by ground-based measurements, and then use the relationship to convert satellite-derived surface $NO_2$ and $NH_3$ concentration ($S_{G\_NH3}*$) to $HNO_3$, $NH_4^+$ and $NO_3^-$ concentrations:

$$\begin{cases} G_{S\_NO3} = S_{G\_NO2} *\times \frac{G_{ACTM\_NO3}}{G_{ACTM\_NO2}} \\ G_{S\_HNO3} = S_{G\_NO2} *\times \frac{G_{ACTM\_HNO3}}{G_{ACTM\_NO2}} \\ G_{S\_NH4} = S_{G\_NH3} *\times \frac{G_{ACTM\_NH4}}{G_{ACTM\_NH3}} \end{cases} \quad (5)$$

$\frac{G_{ACTM\_NO3}}{G_{ACTM\_NO2}}$, $\frac{G_{ACTM\_HNO3}}{G_{ACTM\_NO2}}$, $\frac{G_{ACTM\_NH4}}{G_{ACTM\_NH3}}$ is the estimated ratio of between $NO_2$ and $NO_3^-$, $NO_2$ and $HNO_3$, $NH_3$ and $NH_4^+$.

### 3.3 Dry Deposition of $N_r$

The resistance of dry $N_r$ deposition mainly comes from three aspects: aerodynamic resistance ($R_a$), quasi laminar sub-layer resistance ($R_b$) and canopy resistance ($R_c$). The $V_d$ can be expressed as

$$V_d = \frac{1}{R_a + R_b + R_c} + v_g \quad (6)$$

$V_g$ is gravitational settling velocity. For gases, the $V_g$ is negligible ($V_g$=0).

Dry $NO_2$, $NO_3^-$, $HNO_3$, and $NH_4^+$ deposition can be calculated by:

$$F = G_S \times V_d \quad (7)$$

Unlike above species, $NH_3$ is bi-directional, presenting both upward and downward fluxes. There is a so-called "canopy compensation point" ($C_o$) controlling dry $NH_3$ deposition. Dry $NH_3$ deposition can be calculated by:

$$F = (G_{S\_NH3} - C_o) \times V_d \quad (8)$$

The calculation of $C_o$ is very complex including the leaf stomatal and soil emission

potentials related to the meteorological factors, the plant growth stage and the canopy type. The satellite-based methods usually neglected this complex process and set $C_o$ as zero (Graaf et al., 2018;Kharol et al., 2018) or set fixed values in each land use type based on ground-based measurements (Jia et al., 2016).

### 3.4 Wet Deposition of $N_r$

The satellite-based estimation of wet $N_r$ deposition can be simplified as the product of the concentration of $N_r$ (C), precipitation (P) and scavenging coefficient (w) (Pan et al., 2012). Satellite $NO_2$ and $NH_3$ can be used to indicate the oxidized $N_r$ and reduced $N_r$; precipitation (P) can be obtained from ground monitoring data or reanalysis data (such as NCEP). However, the scavenging coefficient (w) is usually highly uncertain. To improve the accuracy of estimation, a mixed-effects model (Liu et al., 2017a;Zhang et al., 2018) is proposed to build the relationship between satellite $NO_2$ and $NH_3$, precipitation and ground monitoring wet $N_r$ deposition:

$$\mathrm{WetN_{ij}} = \alpha_j + \beta_i \times \mathrm{P_{ij}} \times (\mathrm{S_{ABL}})_{ij} + \varepsilon_{ij} \quad (9)$$

$$\mathrm{S_{ABL}} = \mathrm{S_{trop}} \times \frac{\int_0^{\mathrm{ABL}} \rho(\mathrm{Z})\mathrm{dx}}{\int_0^{\mathrm{h_{trop}}} \rho(\mathrm{Z})\mathrm{dx}} \quad (10)$$

$\mathrm{WetN_{ij}}$ is wet $NO_3^-$N or $NH_4^+$-N deposition at month i and site j; $(\mathrm{S_{ABL}})_{ij}$ is the atmospheric boundary layer (ABL) $NO_2$ or $NH_3$ columns at month i and site j; $\mathrm{P_{ij}}$ is precipitation at month i and site j; $\beta_i$ and $\alpha_j$ are the slope and intercept of random effects, representing seasonal variability and spatial effects; $\varepsilon_{ij}$ represents the random error at month i and site j.

The scavenging process of wet $N_r$ deposition usually starts from the height of rainfall rather than the top of the troposphere, so it is more reasonable to use $NO_2$ and $NH_3$ column below the height of rainfall to build the wet $N_r$ deposition model. The $NO_2$ and $NH_3$ column within ABL is used to build the wet deposition model since

precipitation height is close to the height of the ABL (generally less than 2-3 km).

## 4. Satellite-derived Surface $N_r$ Concentration and Deposition

### 4.1 Surface $NO_2$ Concentration and Oxidized $N_r$ Deposition

The spatial resolutions of global ACTMs and therefore modeled surface $N_r$ concentration are very coarse (for example, the spatial resolution of the global version of GEOS-Chem is $2^o \times 2.5^o$). Thus it can be hard to estimate surface $N_r$ concentration and deposition at a fine resolution at a global scale by ACTMs alone. Instead, the satellite $N_r$ retrievals have a high spatial resolution and can reveal more spatial details than ACTM simulations.

Cheng et al. and Jia et al. established a linear model between the surface $NO_2$ concentration and $NO_2$ column by assuming the ratio of the surface $NO_2$ concentration to the tropospheric $NO_2$ column to be fixed, and then used the linear model to convert satellite $NO_2$ columns to surface $NO_2$ concentration, and finally estimated dry $NO_2$ deposition using the inferential method (Cheng et al., 2013;Jia et al., 2016). However, these statistical methods are highly dependent on the ground-based measurements, and the established linear models may be not effective over regions with few monitoring sites.

A comprehensive study (Nowlan et al., 2014) estimated global surface $NO_2$ concentration during 2005-2007 by multiplying OMI tropospheric $NO_2$ columns by the ACTM-modeled ratio between surface $NO_2$ concentration and tropospheric column (**Fig. 2**). Nowlan et al. also estimated dry $NO_2$ deposition using the OMI-derived surface $NO_2$ concentration combining the modeled $V_d$ during 2005-2007 (Nowlan et al., 2014). This approach followed an earlier study (Lamsal et al., 2008), that focus on North America. As reported by Lamsal et al., the satellite-derived surface $NO_2$ concentration was generally lower than ground-based $NO_2$ observations,

ranging from -17% to -36% in North America (Lamsal et al., 2008). Kharol et al. used a similar method and found the satellite-derived surface $NO_2$ concentration was only half of the ground-measured values in North America (Kharol et al., 2015).

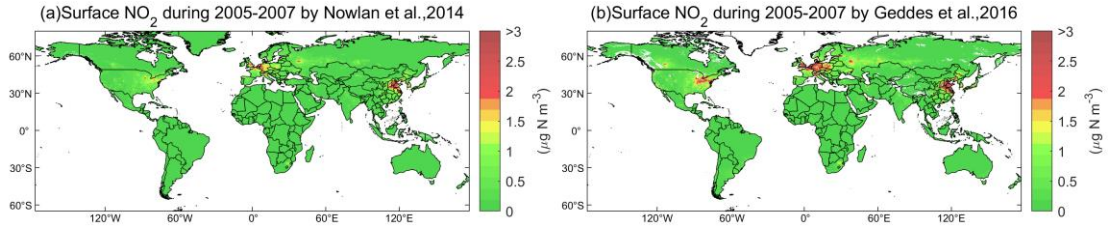


**Fig. 2** Satellite-derived surface $NO_2$ concentration during 2005-2007 by Nowlan et al. (Nowlan et al., 2014) (a) and by Geddes et al. (Geddes et al., 2016) (b). We gained the surface $NO_2$ concentration by Nowlan et al. (Nowlan et al., 2014) and by Geddes et al. (Geddes et al., 2016) at the web: http://fizz.phys.dal.ca/~atmos/martin/?page_id=232.

Geddes et al. followed previous studies, and used $NO_2$ column from the GOME, SCIAMACHY, and GOME-2 to estimate surface $NO_2$ concentration (Geddes et al., 2016). Although Geddes et al. did not evaluate their results with ground-based observation (Geddes et al., 2016), it is obvious that their surface $NO_2$ estimates were higher than Nowlan's estimates based on OMI (Nowlan et al., 2014) (**Fig. 2**). This may be because the OMI-derived $NO_2$ column is much lower than that derived by GOME, SCIAMACHY, and GOME-2, especially over polluted regions. For example, in China, the OMI $NO_2$ column is about 30% lower than that of SCIAMACHY and GOME-2 consistently (**Fig. 3**).

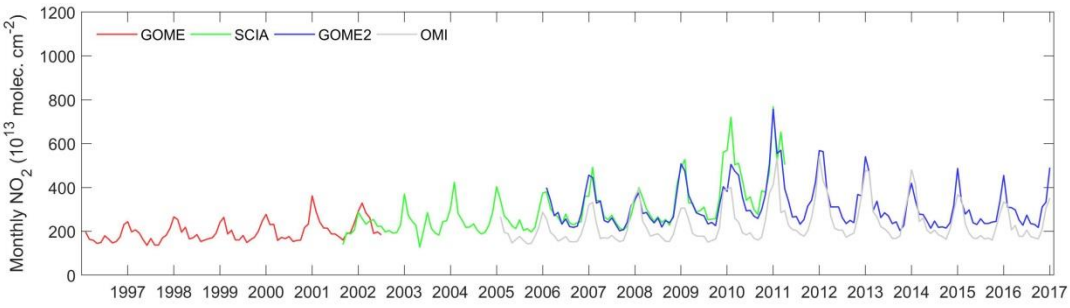


**Fig. 3** An example of the time series of monthly $NO_2$ column retrieved by GOME, SCIAMACHY, GOME2 and OMI in China. We obtained the GOME, SCIAMACHY, GOME2 and OMI data from http://www.temis.nl/airpollution/no2.html.

Larkin et al. established a land-use regression model to estimate global surface $NO_2$

concentration by combining satellite-derived surface $NO_2$ concentration by Geddes et al. and ground-based annual $NO_2$ measurements (Geddes et al., 2016;Larkin et al., 2017). The study by Larkin et al. can be considered as using the ground-based annual measurements to adjust the satellite-derived surface $NO_2$ concentration by Geddes et al. (Geddes et al., 2016;Larkin et al., 2017), which helped reduce the discrepancy between satellite-derived and ground-measured $NO_2$ concentration. The regression model captured 54% of global $NO_2$ variation, with an absolute error of 2.32 μg N $m^{-3}$. Zhang et al. followed the framework in **Sect. 3** to estimate the OMI-derived surface $NO_2$ concentration (at ~50 m) in China, and found good agreement with ground-based surface $NO_2$ concentration from the NNDMN at yearly scale (slope=1.00, $R^2$=0.89) (Zhang et al., 2017). The methods by Zhang et al. can also generate OMI-derived $NO_2$ concentration at any height by the constructed $NO_2$ vertical profile (Zhang et al., 2017). Zhang et al. also estimated dry $NO_2$ deposition using the OMI-derived surface $NO_2$ concentration combining the modeled $V_d$ during 2005-2016 (Zhang et al., 2017). Based on Zhang's estimates, the Gaussian function can well simulate the vertical distribution of $NO_2$ from an ACTM (MOZART) (Emmons et al., 2010) with 99.64% of the grids having $R^2$ values higher than 0.99. This suggests that the ACTM-simulated vertical distribution of $NO_2$ has a general pattern, which can be emulated by Gaussian functions. Once a vertical profile was constructed, it can be easily used to estimate $NO_2$ concentration at any height.

In this study, we used the framework in **Sect. 3** to estimate the OMI-derived surface $NO_2$ concentration globally. To validate the OMI-derived surface $NO_2$ concentrations, ground-measured surface $NO_2$ concentration in China, the US and Europe in 2014 was collected (**Fig. 4**). The total number of $NO_2$ observations in China, the US and Europe are 43, 373 and 88 respectively. The OMI-derived annual average for all sites

was 3.74 μg N $m^{-3}$, which was close to the measured average (3.06 μg N $m^{-3}$). The $R^2$ between OMI-derived surface $NO_2$ concentrations and ground-based $NO_2$ measurements was 0.75 and the RMSE was 1.23 μg N $m^{-3}$ (**Fig. 5**), which is better than the modeling results by the GEOS-Chem ACTM ($R^2$=0.43, RMSE=1.93 μg N $m^{-3}$). Satellite-based methods have the advantages of spatiotemporally continuous monitoring $N_r$ at a higher resolution, which helps alleviate the problem of the coarse resolution of ACTMs in estimating $N_r$ concentration and deposition.

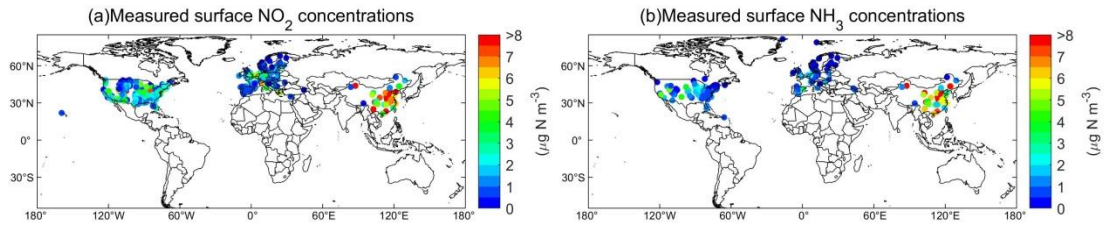


**Fig. 4** Spatial distribution of measured surface $NO_2$ and $NH_3$ concentrations in 2014. For $NO_2$ (a), the measured data in China, the US and Europe were obtained from the NNDMN, US-EPA and EMEP, respectively; for $NH_3$ (b), the measured data in China, the US and Europe were obtained from the NNDMN, US-AMoN and EMEP, respectively

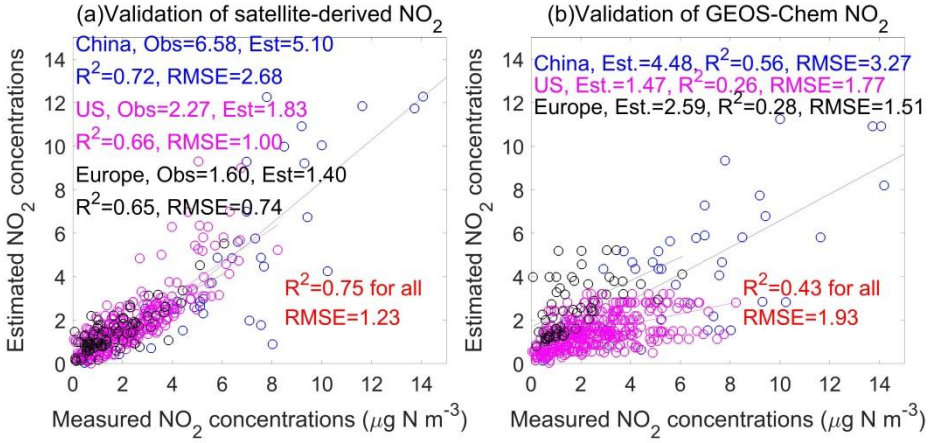


**Fig. 5** Comparison between annual mean satellite-derived and ground-measured surface $NO_2$ concentrations (a), and comparison between annual mean modeled (by an ACTM as GEOS-Chem) and ground-measured surface $NO_2$ concentrations (b). The ground-based monitoring sites are shown in **Fig. 4**.

For $NO_3^-$ and $HNO_3$, previous studies firstly constructed the relationship between $NO_2$, $NO_3^-$ and $HNO_3$, and found a relatively high linear relationship between $NO_2$, $NO_3^-$, and $HNO_3$ at a monthly or yearly scale. For example, Jia et al. found a linear

463 relationship between $NO_2$ and $NO_3^-$, $HNO_3$ concentration at annual scale ($R^2$=0.70)
464 (Jia et al., 2016). Similarly, based on the ground-based measurements in the NNDMN,
465 a high correlation was found between surface $NO_2$ and $NO_3^-$ concentration at monthly
466 or annual timescales (**Fig. 6**) (Liu et al., 2017c). Using these linear relationships and
467 satellite-derived surface $NO_2$ concentration, the annual mean surface $NO_3^-$ and $HNO_3$
468 can be estimated. Alternatively, the relationship of $NO_2$, $NO_3^-$ and $HNO_3$ can also be
469 modeled by an ACTM. For example, a strong relationship of tropospheric $NO_2$, $NO_3^-$
470 and $HNO_3$ column was simulated over all months by an ACTM, with the correlation
471 ranging from 0.69 to 0.91 (Liu et al., 2017a). But, over shorter timescales, the
472 relationship between $NO_2$, $NO_3^-$ and $HNO_3$ may be nonlinear, which we should be
473 cautious about when estimating surface $NO_3^-$ and $HNO_3$ concentration from $NO_2$
474 concentration.

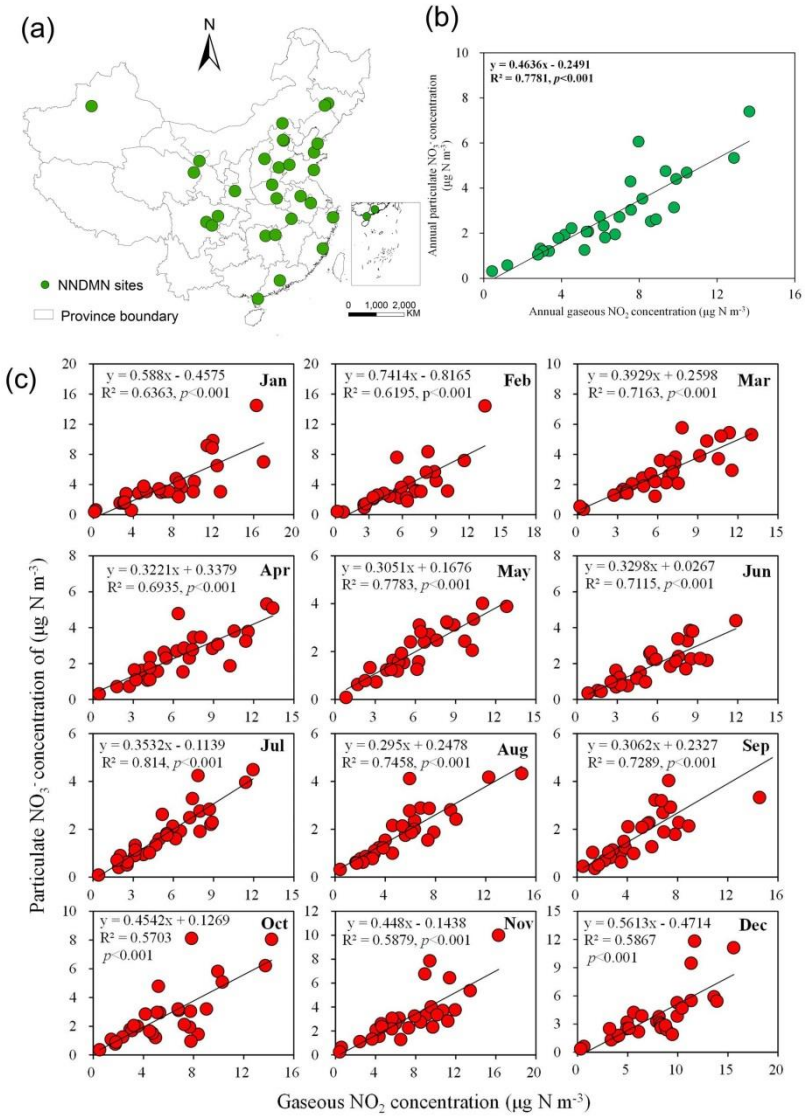


**Fig. 6** Correlation between surface $NO_2$ and particulate $NO_3^-$ concentration in the NNDMN at annual and monthly scales, which were adopted from our previous study (Liu et al., 2017c). (a) indicates the spatial locations of monitoring sites in the NNDMN; (b) and (c) represent yearly and monthly relationship between surface $NO_2$ and particulate $NO_3^-$ concentration, respectively.

For the wet $N_r$ deposition, Liu et al. followed the framework in **Sect. 3** to estimate wet nitrate deposition using ABL $NO_2$ columns derived from OMI $NO_2$ column and $NO_2$ vertical profile from an ACTM (MOZART), and precipitation by a mixed-effects model showing the proposed model can achieve high predictive power for monthly wet nitrate deposition over China (R=0.83, RMSE=0.72) (Liu et al., 2017a).

### 4.2 Surface $NH_3$ Concentration and Reduced $N_r$ Deposition

With the development of atmospheric remote sensing of $NH_3$, some scholars have

estimated surface $NH_3$ concentration and dry $NH_3$ deposition based on the satellite $NH_3$ column data. Assuming the ratio between the surface $NH_3$ concentration to the $NH_3$ column was fixed, Yu et al. applied a linear model to convert satellite $NH_3$ columns to surface $NH_3$ concentration and estimated dry $NH_3$ deposition in China using the inferential method (Yu et al., 2019). But Yu et al. did not consider the spatial variability of the vertical profiles of $NH_3$ (Yu et al., 2019), which may cause a large uncertainty in estimating surface $NH_3$ concentration.

In Western Europe, Graaf et al. used the ratio of the surface $NH_3$ concentration (in the bottom layer) to total $NH_3$ column from an ACTM to convert the IASI $NH_3$ column to surface $NH_3$ concentration, and then estimated dry $NH_3$ deposition combining the modeled deposition velocity and IASI-derived surface $NH_3$ concentration (Graaf et al., 2018). Similarly, in North America, Kharol et al. estimated the dry $NH_3$ deposition by the CrIS-derived surface $NH_3$ concentration and deposition velocity of $NH_3$ (Kharol et al., 2018). They found a relatively high correlation (R=0.76) between the CrIS-derived surface $NH_3$ concentration and AMoN measurements during warm seasons (from April to September) in 2013 (**Fig. 7**). Over China, Liu et al. found a higher correlation (R=0.81) between IASI-derived surface $NH_3$ concentrations and the measured surface $NH_3$ concentrations than those from an ACTM (R=0.57, **Fig. 8**) (Liu et al., 2017b).

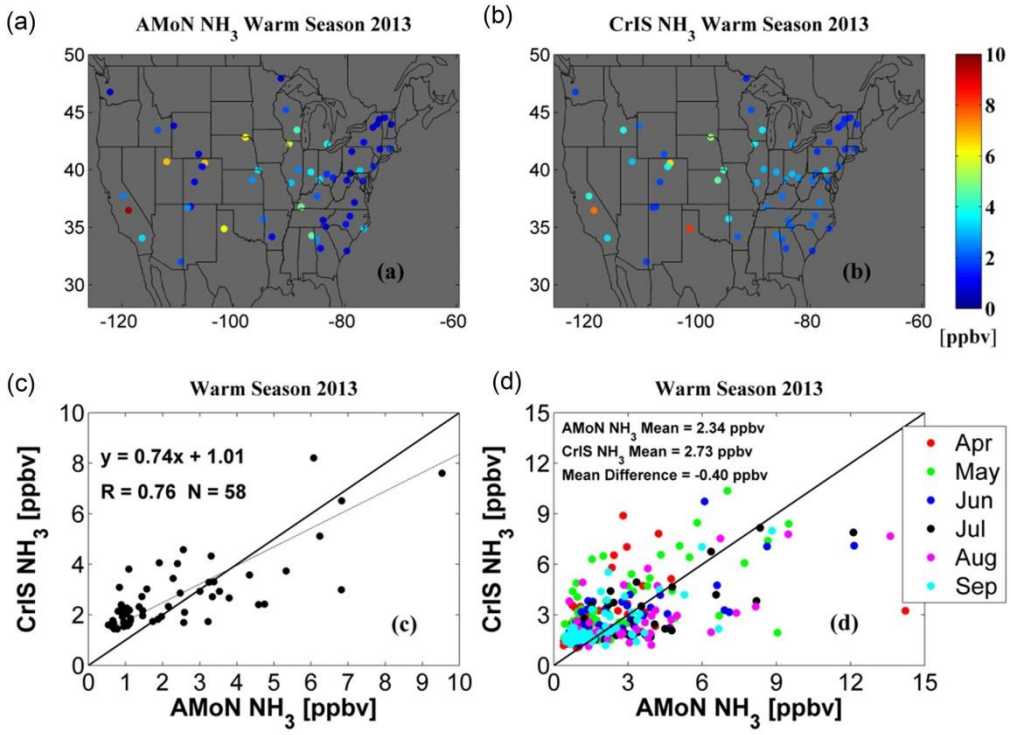


507

508 **Fig. 7** Comparisons of the measured surface $NH_3$ concentration by the AMoN and CrIS-derived
509 surface $NH_3$ concentration in the US during warm season (April-September) in 2013 (Kharol et al.,
510 2018). (a) and (b) indicate measured and CrIS-derived surface $NH_3$ concentration at the AMoN
511 sites, respectively; (c) represents the comparison of averaged surface $NH_3$ concentration during
512 warm months between CrIS-derived estimates and measurements, while (d) indicates the
513 comparison of monthly surface $NH_3$ concentration between CrIS-derived estimates and
514 measurements.
515

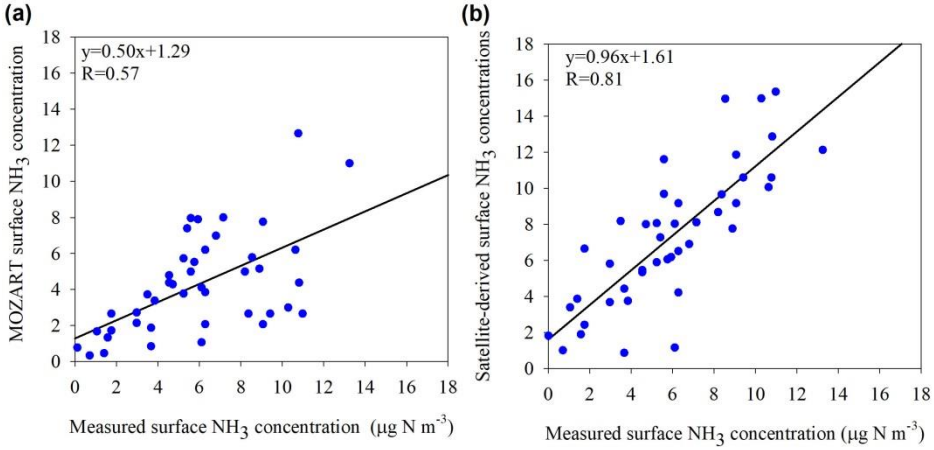


516

517 **Fig. 8** Comparisons of the measured surface $NH_3$ concentration with IASI-derived surface $NH_3$
518 concentration at the NNDMN sites over China (Liu et al., 2017b). (a) indicates the comparison of
519 measured and modeled surface $NH_3$ concentration from an ACTM (MOZART), and (b) represents
520 the comparison of the measured and IASI-derived surface $NH_3$ concentration.
521

522 Liu et al. followed the framework in **Sect. 3** to estimate the IASI-derived surface $NH_3$

523 concentration (at the middle height of the first layer by an ACTM) (**Fig. 9**), and found

a good agreement with ground-based surface $NH_3$ concentration (Liu et al., 2019). The correlation between the measured and satellite-derived annual mean surface $NH_3$ concentrations over all sites was 0.87 as shown in **Fig. 10**, while the average satellite-derived and ground-measured surface $NH_3$ concentration was 2.52 and 2.51 μg N $m^{-3}$ in 2014 at the monitoring sites, respectively. The satellite-derived estimates achieved a better accuracy ($R^2$=0.76, RMSE = 1.50 μg N $m^{-3}$) than an ACTM (GEOS-Chem, $R^2$=0.54, RMSE = 2.14 μg N $m^{-3}$). The satellite $NH_3$ retrievals were affected by the detection limits of the satellite instruments and thermal contrast. Higher correlation over China than other regions for the satellite estimates was linked to the detection limits by the instruments and thermal contrast (Liu et al., 2019). Higher accuracy could be gained with higher thermal contrast and $NH_3$ abundance. Instead, the uncertainties of $NH_3$ retrievals would be higher with lower thermal contrast and $NH_3$ abundance.

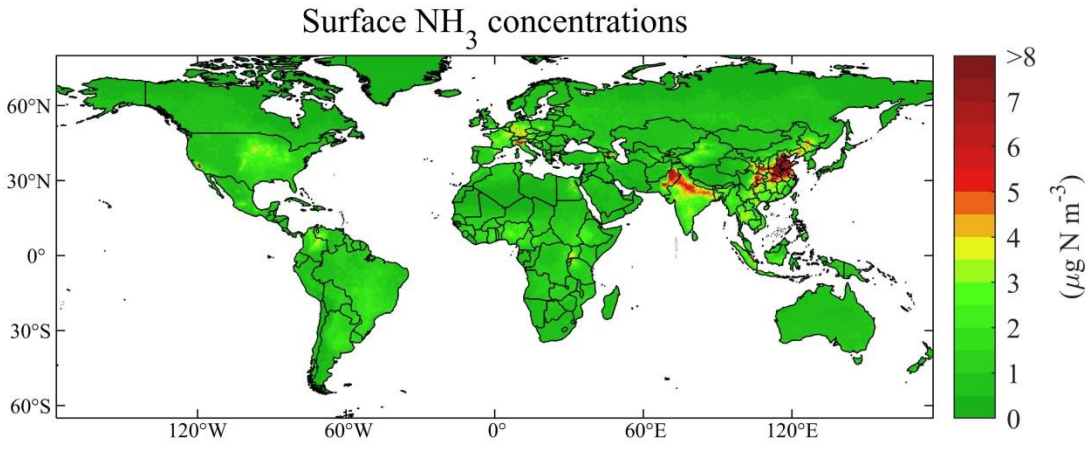


**Fig. 9** Spatially satellite-based surface $NH_3$ estimates in 2014 (Liu et al., 2019). The global surface $NH_3$ concentration datasets have been released on the website: https://zenodo.org/record/3546517#.Xj6I4GgzY2w.

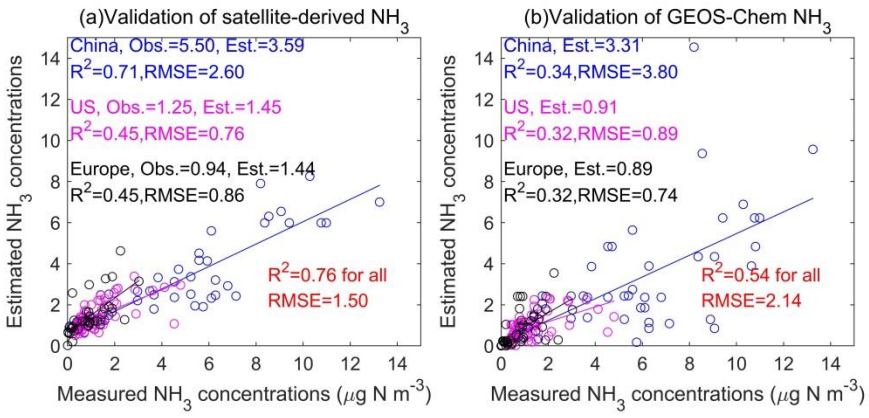


542

543 **Fig. 10** Comparison between yearly satellite-based and measured surface $NH_3$ concentrations (a),
544 and comparison between yearly modeling (by an ACTM as GEOS-Chem) and measured surface
545 $NH_3$ concentrations (b) (Liu et al., 2019). The ground-based monitoring sites are shown in **Fig. 4**.
546

547 The proposed methods (Liu et al., 2019) can also estimate $NH_3$ concentration at any
548 height using the constructed vertical profile function of $NH_3$. The Gaussian function
549 can well emulate the vertical distribution of $NH_3$ from an ACTM outputs with 99% of
550 the grids having $R^2$ values higher than 0.90 (**Fig. 11**). This means, for regional and
551 global estimation, the vertical distribution of $NH_3$ concentration has a general pattern,
552 which can be mostly emulated by the Gaussian function. Once a global $NH_3$ vertical
553 profile was simulated, it can be easily used to estimate satellite-derived $NH_3$
554 concentration at any height. We can also estimate dry $NH_3$ deposition using the
555 IASI-derived surface $NH_3$ concentration combining the modeled $V_d$. For the dry
556 deposition, the uncertainty mainly came from the satellite-derived estimates using the
557 modeled vertical profiles. The uncertainty of vertical profiles modeled by the ACTM
558 mainly resulted from the chemical and transport mechanisms. We recommend using
559 the Gaussian function to determine the height of surface $NO_2$ and $NH_3$ concentrations
560 that best matched with the ground-based measurements. There may exist systematic
561 biases by simply using the relationship of $NO_2$ columns and surface concentration to
562 estimate satellite surface $NO_2$ concentrations. To date, there are still no studies

developing satellite-based methods to estimate the wet reduced $N_r$ deposition on a regional scale.

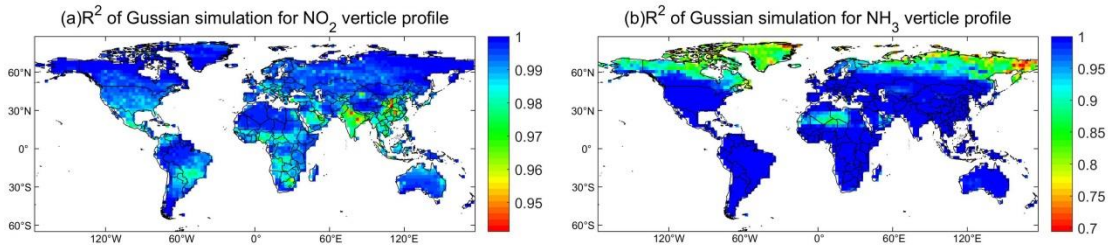


**Fig. 11** Spatial distributions of $R^2$ for Gaussian function by simulating $NH_3$ and $NO_2$ vertical profiles. This is an example of Gaussian fitting using 47 layers' $NH_3$ and $NO_2$ concentration from an ACTM (GEOS-Chem).

## 5. Trends of Surface $N_r$ Concentration and Deposition by Satellite-based Methods

The $N_r$ concentration and deposition modeled by ACTMs are highly dependent on the accuracy of input $N_r$ emissions. The methods commonly used to estimate anthropogenic $N_r$ emissions are based on the data of human activities and emission factors, which can be highly uncertain. The ACTM methods driven by $N_r$ emission inventory have relatively poor timeliness, and have limitations in monitoring the recent trends of $N_r$ deposition.

Satellite-based methods provide a simple, fast and relatively objective way to monitoring $N_r$ deposition at a high resolution, and less susceptible to the errors in the assumptions that emission inventories are compiled based on, particularly the lack of reliable data over developing countries (Crippa et al., 2018). With such advantages, researchers developed the satellite-based methods to estimate surface $N_r$ concentration, deposition and even emissions. Satellite-based methods have advantages in monitoring the recent trends of $N_r$ deposition. Geddes et al. used $NO_2$ column from the GOME, SCIAMACHY, and GOME-2 to estimate satellite-derived $NO_x$ emissions, and then used the calibrated $NO_x$ emission inventory to drive an ACTM to simulate the long-term oxidized $N_r$ deposition globally (Geddes and Martin, 2017). They found

588 oxidized $N_r$ deposition from 1996 to 2014 decreased by 60% in Eastern US, doubled
589 in East China, and declined by 20% in Western Europe (**Fig. 12**). We use the datasets
590 by Geddes et al. to calculate the trends of total oxidized $N_r$ deposition during
591 1996-2014 (Geddes and Martin, 2017). It is obvious that two completely opposite
592 trends exist: (1) in East China with a steep increase of higher than 0.5 kg N $ha^{-1}$ $y^{-1}$
593 and (2) East US with a steep decrease of lower than -0.5 kg N $ha^{-1}$ $y^{-1}$. Although it is
594 not a direct way to use satellite $N_r$ observation to estimate $N_r$ deposition, the method
595 of estimating trends of $N_r$ deposition by Geddes et al. can be considered effective
596 since it took account of the changes of both $NO_x$ emission and climate by an ACTM
597 (Geddes and Martin, 2017).

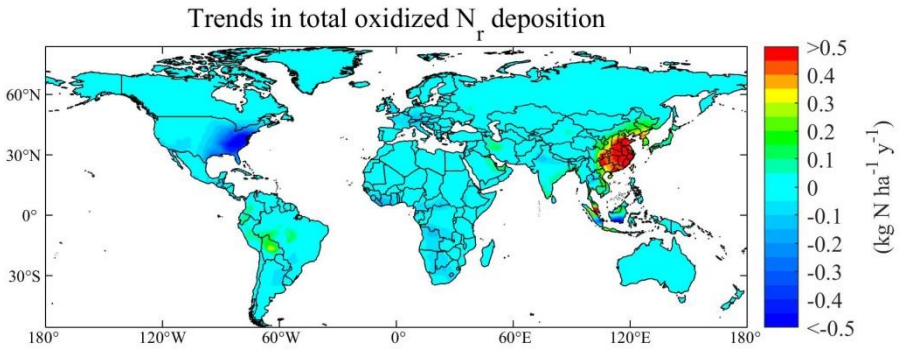


598

599 **Fig. 12** Gridded annual changes of total oxidized $N_r$ deposition simulated by GEOS-Chem
600 constrained with GOME, SCIAMACHY, and GOME-2 $NO_2$ retrievals during 1996-2014 (Geddes
601 and Martin, 2017). We gained the generated datasets
602 (http://fizz.phys.dal.ca/~atmos/martin/?page_id=1520) by Geddes et al., and calculated the trends
603 using the linear methods.
604

605 Some researchers developed a more direct way to infer the trends of surface $N_r$
606 concentration and deposition. Geddes et al. presented a comprehensive long-term
607 global surface $NO_2$ concentration estimate (at 0.1 ° resolution using an oversampling
608 approach) between 1996 and 2012 by using $NO_2$ column from the GOME,
609 SCIAMACHY, and GOME-2 (Geddes et al., 2016). The surface $NO_2$ concentration in
610 North America (the US and Canada) decreased steeply, followed by Western Europe,
611 Japan and South Korea, while approximately tripled in China and North Korea

(Geddes et al., 2016). Jia et al. established a simple linear regression model based on OMI $NO_2$ column and ground-based surface $N_r$ concentration, and then estimated the trends of dry $N_r$ deposition globally between 2005 and 2014 (Jia et al., 2016). They found that dry $N_r$ deposition in Eastern China increased rapidly, while in the Eastern US, Western Europe, and Japan dry $N_r$ deposition has decreased in recent decades.

We split the time span of 2005-2016 into two periods: 2005-2011 and 2011-2016, as surface $NO_2$ concentration shows opposite trend in China in these two periods. The magnitudes of both growth and decline in surface $NO_2$ concentration in China are most pronounced worldwide in the two periods (**Fig. 13**). During 2005-2011, apart from Eastern China with the largest increase in surface $NO_2$ concentration, there are also several areas with increasing trends such as Northwest and East India (New Delhi and Orissa), Western Russia, Eastern Europe (Northern Italy), Western US (Colorado and Utah), Northwestern US (Seattle and Portland), Southwestern Canada (Vancouver, Edmonton, Calgary), Northeast Pakistan and Northwest Xinjiang (Urumqi). Notably, the biggest decreases in surface $NO_2$ concentration during 2005-2011 occurred in Eastern US and Western EU (North France, South England, and West German). During 2011-2016, due to the strict control of $NO_x$ emissions, Eastern China had the largest decrease in surface $NO_2$ concentration than elsewhere worldwide, followed by Western Xinjiang, Western Europe and some areas in Western Russia.

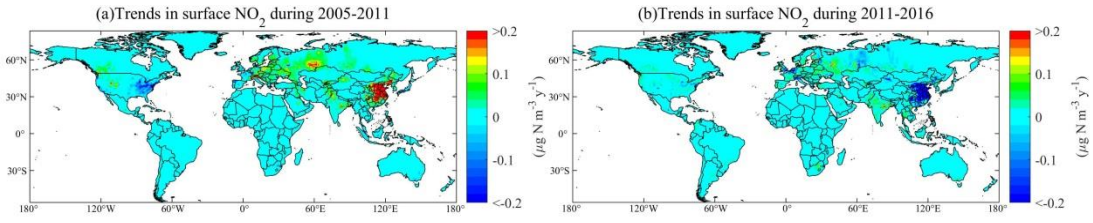


**Fig. 13** Gridded annual changes in surface $NO_2$ concentrations gained by OMI retrievals during 2005-2011 (a) and during 2011-2016 (b) in this study. We have released the global surface $NO_2$ concentrations during 2005-2016 available at the website: https://zenodo.org/record/3546517#.Xj6I4GgzY2w.

Liu et al. estimated surface $NH_3$ concentration globally during 2008-2016 using

satellite $NH_3$ retrievals by IASI (Liu et al., 2019). A large increase of surface $NH_3$ concentrations was found in Eastern China, followed by Northern Xinjiang province in China during 2008-2016 (**Fig. 14**). Satellite-based methods have been proven as an effective and unique way to monitoring the trends of global $N_r$ concentration and deposition. To date, there are still few studies reporting the satellite-derived trends of reduced $N_r$ deposition on a global scale.

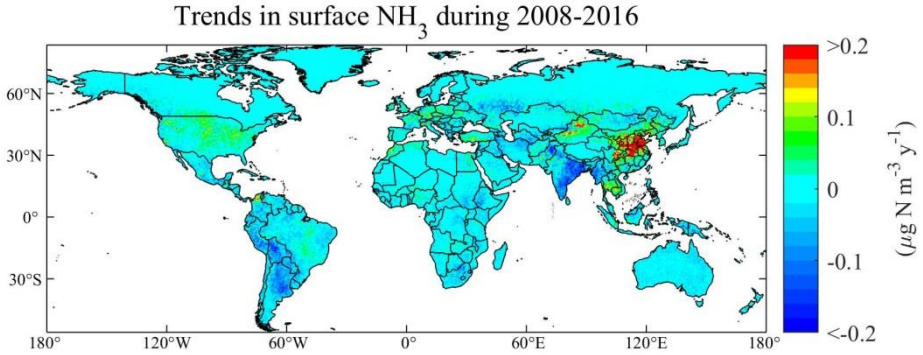


**Fig. 14** Gridded annual changes in surface $NH_3$ concentrations gained by IASI retrievals during 2008-2016 (Liu et al., 2019). We have released the global surface $NH_3$ concentrations during 2008-2016 at the website: https://zenodo.org/record/3546517#.Xj6I4GgzY2w.

## 6. Remaining Challenges for Estimating $N_r$ Deposition Using Satellite Observation

First, the reduced $N_r$ deposition plays an important contribution to total $N_r$ deposition. $NH_3$ exhibits bi-directional air-surface exchanges. The $NH_3$ compensation point (Farquhar et al., 1980) is also an important and highly variable factor controlling dry $NH_3$ deposition (Schrader et al., 2016;Zhang et al., 2010). However, the current existing satellite-based methods did not consider this bi-directional air-surface exchange. It is important to better parameterize the $NH_3$ compensation point, and assess the effects of bi-directional air-surface exchanges on estimating the dry $NH_3$ deposition.

Second, the existing satellite-based methods to estimate $N_r$ deposition used the ratio of the surface $N_r$ concentration to the $N_r$ column by an ACTM to convert satellite $N_r$

column to surface $N_r$ concentration. However, the calculated ratio (by an ACTM) and the satellite $N_r$ column have different spatial resolutions, and previous studies usually applied the modeled ratio directly or interpolate the ratio into the resolution of satellite $N_r$ column. This method assumes the relationship at coarse resolution by an ACTM can also be effective in fine resolution as satellite indicated. When regional studies are conducted, regional ACTMs coupled with another meteorological model (e.g. WRF-Chem, WRF-CMAQ) (Grell et al., 2005;Wong et al., 2012) can be configured to match the spatial resolution of satellite observation, but this is not as viable for global ACTMs (e.g. MOZART, GEOS-Chem) due to differences in model structures and computational cost. The modeled ratio of surface $N_r$ concentration to the $N_r$ column may have variability at spatial scales finer than the horizontal resolution of global ACTMs. The impact of such scale effect (at different spatial scales) on estimated surface $N_r$ concentration should be further studied.

Third, the satellite observation can only obtain reliable $NO_2$ and $NH_3$ column presently, and there are no available high-resolution and reliable direct $HNO_3$, $NO_3^-$, $NH_4^+$ retrievals. For $HNO_3$, $NO_3^-$, $NH_4^+$ concentrations, the satellite-based methods often applied the satellite-derived $NO_2$ and $NH_3$ concentration and the relationship between $N_r$ species from an ACTM (or ground-based measurements) to estimate surface $HNO_3$, $NO_3^-$, $NH_4^+$ concentration. With the development of satellite technology, more and more $N_r$ species can be detected, such as $HNO_3$. However, at present, satellite $HNO_3$ products are not mature, and the spatial resolution is low. Direct, high-resolution and reliable satellite monitoring of more $N_r$ species is critical to further developing the use of using atmospheric remote sensing to estimate $N_r$ deposition at global and regional scales.

Fourth, estimating wet $N_r$ deposition using satellite $NO_2$ and $NH_3$ column remains

relatively uncommon. Further studies should focus on how to combine the high-resolution satellite $NO_2$ and $NH_3$ column and the ground-based monitoring data to build wet $N_r$ deposition models to estimate wet $N_r$ deposition at higher spatiotemporal resolution. The proposed scheme to estimate the wet $N_r$ deposition in **Sect. 3** is statistical. On the other hand, the wet $N_r$ deposition includes the scavenging processes of in-cloud, under-cloud and precipitation. Processed-level knowledge and models can benefit the estimation of wet $N_r$ deposition using satellite $NO_2$ and $NH_3$ column.

## 7. Conclusion

The recent advances of satellite-based methods for estimating surface $N_r$ concentration and deposition have been reviewed. Previous studies have focused on using satellite $NO_2$ column to estimate surface $NO_2$ concentrations and dry $NO_2$ deposition both regionally and globally. The research on calculating surface $NH_3$ concentration and reduced $N_r$ deposition by satellite $NH_3$ data is just beginning, and some scholars have carried out estimating surface $NH_3$ concentration and dry $NH_3$ deposition on different spatial and temporal scales, but the research degree is still relatively low. We present a framework of using satellite $NO_2$ and $NH_3$ column to estimate $N_r$ deposition based on recent advances. The proposed framework of using Gaussian function to model vertical $NO_2$ and $NH_3$ profiles can be used to convert the satellite $NO_2$ and $NH_3$ column to surface $NO_2$ and $NH_3$ concentration at any height simply and quickly. The proposed framework of using satellite $NO_2$ and $NH_3$ column to estimate wet $N_r$ deposition is a statistical way, and further studies should be done from a mechanism perspective. Finally, we summarized current challenges of using satellite $NO_2$ and $NH_3$ column to estimate surface $N_r$ concentration and deposition including a lack of considering $NH_3$ bidirectional air-surface exchanges and the

problem of different spatial scales between an ACTM and satellite observation.

**Acknowledgments**

This study is supported by the National Natural Science Foundation of China (No. 41471343, 41425007 and 41101315) and the Chinese National Programs on Heavy Air Pollution Mechanisms and Enhanced Prevention Measures (Project No. 8 in the 2nd Special Program).

**Author contributions**. LL designed this study. LL, YYY and WX conducted the data analysis. All co-authors contributed to the revision of the paper.

**Data availability**. OMI $NO_2$ datasets are available at http://www.temis.nl/airpollution/no2.html. IASI $NH_3$ datasets are available at https://cds-espri.ipsl.upmc.fr/etherTypo/index.php?id=1700&L=1. Surface $NO_2$ concentration during 2005-2007 obtained by Nowlan et al. (Nowlan et al., 2014) and longterm estimates (1996-2012) by Geddes et al. (Geddes et al., 2016) are available at http://fizz.phys.dal.ca/~atmos/martin/?page_id=232. Total oxidized $N_r$ deposition simulated by GEOS-Chem constrained with GOME, SCIAMACHY, and GOME-2 $NO_2$ retrievals during 1996-2014 (Geddes and Martin, 2017) is available at http://fizz.phys.dal.ca/~atmos/martin/?page_id=1520. A database of atmospheric $N_r$ concentration and deposition from the nationwide monitoring network in China is available at https://www.nature.com/articles/s41597-019-0061-2. Measured $N_r$ concentration and deposition datasets in the United States are available on the website: https://www.epa.gov/outdoor-air-quality-data. Measured surface $NO_2$ and $NH_3$ concentration datasets in Europe are available at https://www.nilu.no/projects/ccc/emepdata.html. Global surface $NO_2$ and $NH_3$ concentration data used to calculate the longterm trends in **Fig. 13** and **Fig. 14** have been released on the website: https://zenodo.org/record/3546517#.Xj6I4GgzY2w.

**Competing interests**. The authors declare no competing financial interests.

## Reference


Amos, H. M., Jacob, D. J., Holmes, C. D., Fisher, J. A., Wang, Q., Yantosca, R. M., Corbitt, E. S., Galarneau, E., Rutter, A. P., and Gustin, M. S.: Gas-particle partitioning of atmospheric Hg(II) and its effect on global mercury deposition, Atmos. Chem. Phys., 11, 29441-29477, 2012.

Beer, R., Shephard, M. W., Kulawik, S. S., Clough, S. A., Eldering, A., Bowman, K. W., Sander, S. P., Fisher, B. M., Payne, V. H., Luo, M., Osterman, G. B., and Worden, J. R.: First satellite observations of lower tropospheric ammonia and methanol, Geophys. Res Lett., 35, 1-5, 10.1029/2008GL033642, 2008.

Bobbink, R., Hicks, K., Galloway, J., Spranger, T., Alkemade, R., Ashmore, M., Bustamante, M., Cinderby, S., Davidson, E., Dentener, F., Emmett, B., Erisman, J.-W., Fenn, M., Gilliam, F., Nordin, A., Pardo, L., and De Vries, W.: Global assessment of nitrogen deposition effects on terrestrial plant diversity: a synthesis, Ecological Applications, 20, 30-59, doi:10.1890/08-1140.1, 2010.

Boersma, K. F., Eskes, H. J., Dirksen, R. J., van der A, R. J., Veefkind, J. P., Stammes, P., Huijnen, V., Kleipool, Q. L., Sneep, M., Claas, J., Leitão, J., Richter, A., Zhou, Y., and Brunner, D.: An improved tropospheric $NO_2$ column retrieval algorithm for the Ozone Monitoring Instrument, Atmospheric Measurement Techniques, 4, 1905-1928, 10.5194/amt-4-1905-2011, 2011.

Canfield, D. E., Glazer, A. N., and Falkowski, P. G.: The evolution and future of Earth's nitrogen cycle, Science, 330, 192-196, 2010.

758 Cao, G. L., Zhang, X. Y., and Gong, S. L.: Emission inventories of primary particles
759 and pollutant gases for China, Science Bulletin, 56, 781-788, 2011.
760 Cheng, M., Jiang, H., Guo, Z., Zhang, X., and Lu, X.: Estimating $NO_2$ dry deposition
761 using satellite data in eastern China, Int. J. Remote Sens., 34, 2548-2565, 2013.
762 Coheur, P.-F., Clarisse, L., Turquety, S., Hurtmans, D., and Clerbaux, C.: IASI
763 measurements of reactive trace species in biomass burning plumes, Atmos. Chem.
764 Phys., 9, 5655-5667, 2009.
765 Crippa, M., Guizzardi, D., Muntean, M., Schaaf, E., Dentener, F., van Aardenne, J. A.,
766 Monni, S., Doering, U., Olivier, J. G. J., Pagliari, V., and Janssens-Maenhout, G.:
767 Gridded emissions of air pollutants for the period 1970–2012 within EDGAR v4.3.2,
768 Earth Syst. Sci. Data, 10, 1987-2013, 10.5194/essd-10-1987-2018, 2018.
769 Dammers, E., Palm, M., Van Damme, M., Vigouroux, C., Smale, D., Conway, S.,
770 Toon, G. C., Jones, N., Nussbaumer, E., Warneke, T., Petri, C., Clarisse, L., Clerbaux,
771 C., Hermans, C., Lutsch, E., Strong, K., Hannigan, J. W., Nakajima, H., Morino, I.,
772 Herrera, B., Stremme, W., Grutter, M., Schaap, M., Wichink Kruit, R. J., Notholt, J.,
773 Coheur, P. F., and Erisman, J. W.: An evaluation of IASI-$NH_3$ with ground-based
774 Fourier transform infrared spectroscopy measurements, Atmos. Chem. Phys., 16,
775 10351-10368, 10.5194/acp-16-10351-2016, 2016.
776 David, F., M, C., U, S., MA, S., JN, C., S, R., LJ, S., A, J., B, G., and JN, G.: The
777 global nitrogen cycle in the twenty-first century, Philosophical Transactions of the
778 Royal Society of London, 368, 20130164, 2013.
779 Emmons, L., Walters, S., Hess, P., Lamarque, J.-F., Pfister, G., Fillmore, D., Granier,

780 C., Guenther, A., Kinnison, D., and Laepple, T.: Description and evaluation of the
781 Model for Ozone and Related chemical Tracers, version 4 (MOZART-4),
782 Geoscientific Model Development, 3, 43-67, 2010.
783 Erisman, J. W., Sutton, M. A., Galloway, J., Klimont, Z., and Winiwarter, W.: How a
784 century of ammonia synthesis changed the world, Nat. Geosci., 1, 636-639, 2008.
785 Farquhar, G. D., Firth, P. M., Wetselaar, R., and Weir, B.: On the Gaseous Exchange
786 of Ammonia between Leaves and the Environment: Determination of the Ammonia
787 Compensation Point, Plant Physiology, 66, 710-714, 10.1104/pp.66.4.710, 1980.
788 Galloway, J. N., Dentener, F. J., Capone, D. G., Boyer, E. W., Howarth, R. W.,
789 Seitzinger, S. P., Asner, G. P., Cleveland, C., Green, P., and Holland, E.: Nitrogen
790 cycles: past, present, and future, Biogeochemistry, 70, 153-226, 2004a.
791 Galloway, J. N., Dentener, F. J., Capone, D. G., Boyer, E. W., Howarth, R. W.,
792 Seitzinger, S. P., Asner, G. P., Cleveland, C. C., Green, P. A., Holland, E. A., Karl, D.
793 M., Michaels, A. F., Porter, J. H., Townsend, A. R., and Vöosmarty, C. J.: Nitrogen
794 Cycles: Past, Present, and Future, Biogeochemistry, 70, 153-226,
795 10.1007/s10533-004-0370-0, 2004b.
796 Galloway, J. N., Townsend, A. R., Erisman, J. W., Bekunda, M., Cai, Z., Freney, J. R.,
797 Martinelli, L. A., Seitzinger, S. P., and Sutton, M. A.: Transformation of the nitrogen
798 cycle: recent trends, questions, and potential solutions, Science, 320, 889-892, 2008.
799 Geddes, J. A., Martin, R. V., Boys, B. L., and van Donkelaar, A.: Long-term trends
800 worldwide in ambient $NO_2$ concentrations inferred from satellite observations,
801 Environmental Health Perspectives, 124, 281, 2016.

802 Geddes, J. A., and Martin, R. V.: Global deposition of total reactive nitrogen oxides
803 from 1996 to 2014 constrained with satellite observations of $NO_2$ columns, Atmos.
804 Chem. Phys., 17, 10071-10091, 2017.
805 Graaf, S. C. v. d., Dammers, E., Schaap, M., and Erisman, J. W.: How are $NH_3$ dry
806 deposition estimates affected by combining the LOTOS-EUROS model with
807 IASI-NH3 satellite observations?, Atmos. Chem. Phys., 18, 13173-13196,
808 https://doi.org/10.5194/acp-2018-133, 2018.
809 Grell, G. A., Peckham, S. E., Schmitz, R., McKeen, S. A., Frost, G., Skamarock, W.
810 C., and Eder, B.: Fully coupled "online" chemistry within the WRF model, Atmos.
811 Environ., 39, 6957-6975, 2005.
812 Hoesly, R. M., Smith, S. J., Feng, L., Klimont, Z., Janssens-Maenhout, G., Pitkanen,
813 T., Seibert, J. J., Vu, L., Andres, R. J., Bolt, R. M., Bond, T. C., Dawidowski, L.,
814 Kholod, N., Kurokawa, J. I., Li, M., Liu, L., Lu, Z., Moura, M. C. P., O'Rourke, P. R.,
815 and Zhang, Q.: Historical (1750–2014) anthropogenic emissions of reactive gases and
816 aerosols from the Community Emissions Data System (CEDS), Geosci. Model Dev.,
817 11, 369-408, 10.5194/gmd-11-369-2018, 2018.
818 Janssens, I. A., Dieleman, W., Luyssaert, S., Subke, J. A., Reichstein, M., Ceulemans,
819 R., Ciais, P., Dolman, A. J., Grace, J., Matteucci, G., Papale, D., Piao, S. L., Schulze,
820 E. D., Tang, J., and Law, B. E.: Reduction of forest soil respiration in response to
821 nitrogen deposition, Nat. Geosci., 3, 315, 10.1038/ngeo844
822 https://www.nature.com/articles/ngeo844#supplementary-information, 2010.
823 Jia, Y., Yu, G., Gao, Y., He, N., Wang, Q., Jiao, C., and Zuo, Y.: Global inorganic

824 nitrogen dry deposition inferred from ground-and space-based measurements,
825 Scientific reports, 6, 1-11, 2016.
826 Kharol, S. K., Martin, R. V., Philip, S., Boys, B., Lamsal, L. N., Jerrett, M., Brauer,
827 M., Crouse, D. L., Mclinden, C., and Burnett, R. T.: Assessment of the magnitude and
828 recent trends in satellite-derived ground-level nitrogen dioxide over North America,
829 Atmos. Environ., 118, 236-245, 2015.
830 Kharol, S. K., Shephard, M. W., McLinden, C. A., Zhang, L., Sioris, C. E., O'Brien, J.
831 M., Vet, R., Cady-Pereira, K. E., Hare, E., Siemons, J., and Krotkov, N. A.: Dry
832 Deposition of Reactive Nitrogen From Satellite Observations of Ammonia and
833 Nitrogen Dioxide Over North America, Geophys. Res Lett., 45, 1157-1166,
834 10.1002/2017GL075832, 2018.
835 Kim, T. W., Lee, K., Duce, R., and Liss, P.: Impact of atmospheric nitrogen deposition
836 on phytoplankton productivity in the South China Sea, Geophys. Res Lett., 41, 3156–
837 3162, 2014.
838 Kuik, F., Lauer, A., Churkina, G., Denier van der Gon, H. A. C., Fenner, D., Mar, K.
839 A., and Butler, T. M.: Air quality modelling in the Berlin-Brandenburg region using
840 WRF-Chem v3.7.1: sensitivity to resolution of model grid and input data,
841 Geoscientific Model Development Discussions, 9, 4339-4363, 2016.
842 Lamarque, J. F., Kiehl, J., Brasseur, G., Butler, T., Cameron‐Smith, P., Collins, W.,
843 Collins, W., Granier, C., Hauglustaine, D., and Hess, P.: Assessing future nitrogen
844 deposition and carbon cycle feedback using a multimodel approach: Analysis of
845 nitrogen deposition, Journal of Geophysical Research: Atmospheres (1984–2012), 110,

2005.

Lamsal, L. N., Martin, R. V., van Donkelaar, A., Steinbacher, M., Celarier, E. A., Bucsela, E., Dunlea, E. J., and Pinto, J. P.: Ground-level nitrogen dioxide concentrations inferred from the satellite-borne Ozone Monitoring Instrument, J. Geophys. Res-Atmos., 113, 1-15, 10.1029/2007JD009235, 2008.

Lamsal, L. N., Martin, R. V., Parrish, D. D., and Krotkov, N. A.: Scaling relationship for $NO_2$ pollution and urban population size: a satellite perspective, Environ. Sci. Technol., 47, 7855-7861, 2013.

Larkin, A., Geddes, J. A., Martin, R. V., Xiao, Q., Liu, Y., Marshall, J. D., Brauer, M., and Hystad, P.: Global Land Use Regression Model for Nitrogen Dioxide Air Pollution, Environ. Sci. Technol., 51, 6957-6964, 2017.

Larssen, T., Duan, L., and Mulder, J.: Deposition and leaching of sulfur, nitrogen and calcium in four forested catchments in China: implications for acidification, Environ. Sci. Technol., 45, 1192-1198, 2011.

Levine, S. Z., and Schwartz, S. E.: In-cloud and below-cloud scavenging of Nitric acid vapor, Atmospheric Environment (1967), 16, 1725-1734, https://doi.org/10.1016/0004-6981(82)90266-9, 1982.

Li, Y., Thompson, T. M., Damme, M. V., Chen, X., Benedict, K. B., Shao, Y., Day, D., Boris, A., Sullivan, A. P., and Ham, J.: Temporal and Spatial Variability of Ammonia in Urban and Agricultural Regions of Northern Colorado, United States, Atmos. Chem. Phys., 17, 1-50, 2017.

Liu, H., Jacob, D. J., Bey, I., and Yantosca, R. M.: Constraints from 210Pb and 7Be on

wet deposition and transport in a global three-dimensional chemical tracer model driven by assimilated meteorological fields, J. Geophys. Res-Atmos., 106, 12109-12128, 10.1029/2000JD900839, 2001.

Liu, L., Zhang, X., Xu, W., Liu, X., Lu, X., Chen, D., Zhang, X., Wang, S., and Zhang, W.: Estimation of monthly bulk nitrate deposition in China based on satellite $NO_2$ measurement by the Ozone Monitoring Instrument, Remote Sens. Environ., 199, 93-106, 2017a.

Liu, L., Zhang, X., Xu, W., Liu, X., Lu, X., Wang, S., Zhang, W., and Zhao, L.: Ground Ammonia Concentrations over China Derived from Satellite and Atmospheric Transport Modeling, Remote Sens., 9, 467, 2017b.

Liu, L., Zhang, X., Zhang, Y., Xu, W., Liu, X., Zhang, X., Feng, J., Chen, X., Zhang, Y., Lu, X., Wang, S., Zhang, W., and Zhao, L.: Dry Particulate Nitrate Deposition in China, Environ. Sci. Technol., 51, 5572-5581, 10.1021/acs.est.7b00898, 2017c.

Liu, L., Zhang, X., Wong, A. Y. H., Xu, W., Liu, X., Li, Y., Mi, H., Lu, X., Zhao, L., Wang, Z., and Wu, X.: Estimating global surface ammonia concentrations inferred from satellite retrievals, Atmos. Chem. Phys., 19, 12051-12066, 10.5194/acp-2019-184, 2019.

Liu, L., Zhang, X., Xu, W., Liu, X., Wei, J., Wang, Z., and Yang, Y.: Global estimates of dry ammonia deposition inferred from space-measurements, Sci.Total Environ., 730, 139189, https://doi.org/10.1016/j.scitotenv.2020.139189, 2020.

Liu, X., Duan, L., Mo, J., Du, E., Shen, J., Lu, X., Zhang, Y., Zhou, X., He, C., and Zhang, F.: Nitrogen deposition and its ecological impact in China: An overview,

Environ. Pollut., 159, 2251-2264, http://dx.doi.org/10.1016/j.envpol.2010.08.002, 2011.

Liu, X., Xu, W., Duan, L., Du, E., Pan, Y., Lu, X., Zhang, L., Wu, Z., Wang, X., Zhang, Y., Shen, J., Song, L., Feng, Z., Liu, X., Song, W., Tang, A., Zhang, Y., Zhang, X., and Collett, J. L.: Atmospheric Nitrogen Emission, Deposition, and Air Quality Impacts in China: an Overview, Curr. Pollut. Rep., 3, 65-77, 10.1007/s40726-017-0053-9, 2017d.

Lu, X., Jiang, H., Zhang, X., Liu, J., Zhang, Z., Jin, J., Wang, Y., Xu, J., and Cheng, M.: Estimated global nitrogen deposition using $NO_2$ column density, Int. J. Remote Sens., 34, 8893-8906, 2013.

Mari, C., Jacob, D. J., and Bechtold, P.: Transport and scavenging of soluble gases in a deep convective cloud, J. Geophys. Res-Atmos., 105, 22255-22268, 2000.

Nadelhoffer, K. J., Emmett, B. A., Gundersen, P., Kjønaas, O. J., Koopmans, C. J., Schleppi, P., Tietema, A., and Wright, R. F.: Nitrogen deposition makes a minor contribution to carbon sequestration in temperate forests, Nature, 398, 145, 10.1038/18205, 1999.

Nemitz, E., Flynn, M., Williams, P. I., Milford, C., Theobald, M. R., Blatter, A., Gallagher, M. W., and Sutton, M. A.: A Relaxed Eddy Accumulation System for the Automated Measurement of Atmospheric Ammonia Fluxes, Water, Air and Soil Pollution: Focus, 1, 189-202, 10.1023/A:1013103122226, 2001.

Nicolas, G., and Galloway, J. N.: An Earth-system perspective of the global nitrogen cycle, Nature, 451, 293-296, 2008.

912 Nowlan, C., Martin, R., Philip, S., Lamsal, L., Krotkov, N., Marais, E., Wang, S., and
913 Zhang, Q.: Global dry deposition of nitrogen dioxide and sulfur dioxide inferred from
914 space-based measurements, Global Biogeochem. Cy., 28, 1025-1043, 2014.
915 Paerl, H. W., Gardner, W. S., Mccarthy, M. J., Peierls, B. L., and Wilhelm, S. W.:
916 Algal blooms: noteworthy nitrogen, Science, 346, 175, 2014.
917 Pan, Y., Wang, Y., Tang, G., and Wu, D.: Wet and dry deposition of atmospheric
918 nitrogen at ten sites in Northern China, Atmos. Chem. Phys., 12, 6515-6535, 2012.
919 Ronsmans, G., Langerock, B., Wespes, C., Hannigan, J. W., Hase, F., Kerzenmacher,
920 T., Mahieu, E., Schneider, M., Smale, D., Hurtmans, D., De Mazière, M., Clerbaux, C.,
921 and Coheur, P. F.: First characterization and validation of FORLI-HNO3 vertical
922 profiles retrieved from IASI/Metop, Atmos. Meas. Tech., 9, 4783-4801,
923 10.5194/amt-9-4783-2016, 2016.
924 Schrader, F., Brümmer, C., Flechard, C. R., Wichink Kruit, R. J., van Zanten, M. C.,
925 Zöll, U., Hensen, A., and Erisman, J. W.: Non-stomatal exchange in ammonia dry
926 deposition models: comparison of two state-of-the-art approaches, Atmos. Chem.
927 Phys., 16, 13417-13430, 10.5194/acp-16-13417-2016, 2016.
928 Shen, J., Li, Y., Liu, X., Luo, X., Tang, H., Zhang, Y., and Wu, J.: Atmospheric dry
929 and wet nitrogen deposition on three contrasting land use types of an agricultural
930 catchment in subtropical central China, Atmos. Environ., 67, 415-424,
931 http://dx.doi.org/10.1016/j.atmosenv.2012.10.068, 2013.
932 Stevens, C. J., Dise, N. B., Mountford, J. O., and Gowing, D. J.: Impact of Nitrogen
933 Deposition on the Species Richness of Grasslands, Science, 303, 1876-1879,

10.1126/science.1094678, 2004.

Sutton, M. A., Tang, Y. S., Miners, B., and Fowler, D.: A New Diffusion Denuder System for Long-Term, Regional Monitoring of Atmospheric Ammonia and Ammonium, Water Air & Soil Pollution Focus, 1, 145-156, 2001.

Sutton, M. A., Bleeker, A., Howard, C. M., Bekunda, M., Grizzetti, B., Vries, W. D., Grinsven, H. J. M. V., Abrol, Y. P., Adhya, T. K., and Billen, G.: Our Nutrient World: the challenge to produce more food and energy with less pollution, 2013.

Tan, J., Fu, J. S., Dentener, F., Sun, J., Emmons, L., Tilmes, S., Sudo, K., Flemming, J., Jonson, J. E., and Gravel, S.: Multi-model study of HTAP II on sulfur and nitrogen deposition, Atmos. Chem. Phys., 18, 1-36, 2018.

Van Damme, M., Clarisse, L., Dammers, E., Liu, X., Nowak, J., Clerbaux, C., Flechard, C., Galy-Lacaux, C., Xu, W., and Neuman, J.: Towards validation of ammonia ($NH_3$) measurements from the IASI satellite, Atmospheric Measurement Techniques, 7, 12125-12172, 2014a.

Van Damme, M., Wichink Kruit, R., Schaap, M., Clarisse, L., Clerbaux, C., Coheur, P. F., Dammers, E., Dolman, A., and Erisman, J.: Evaluating 4 years of atmospheric ammonia ($NH_3$) over Europe using IASI satellite observations and LOTOS-EUROS model results, J. Geophys. Res-Atmos., 119, 9549-9566, 2014b.

Van der Graaf, S. C., Dammers, E., Schaap, M., and Erisman, J. W.: Technical note: How are $NH_3$ dry deposition estimates affected by combining the LOTOS-EUROS model with IASI-$NH_3$ satellite observations?, Atmos. Chem. Phys., 18, 13173-13196, 10.5194/acp-18-13173-2018, 2018.

956 Vet, R., Artz, R. S., Carou, S., Shaw, M., Ro, C.-U., Aas, W., Baker, A., Bowersox, V.
957 C., Dentener, F., Galy-Lacaux, C., Hou, A., Pienaar, J. J., Gillett, R., Forti, M. C.,
958 Gromov, S., Hara, H., Khodzher, T., Mahowald, N. M., Nickovic, S., Rao, P. S. P., and
959 Reid, N. W.: A global assessment of precipitation chemistry and deposition of sulfur,
960 nitrogen, sea salt, base cations, organic acids, acidity and pH, and phosphorus, Atmos.
961 Environ., 93, 3-100, http://dx.doi.org/10.1016/j.atmosenv.2013.10.060, 2014.
962 Vitousek, P. M., Aber, J. D., Howarth, R. W., Likens, G. E., Matson, P. A., Schindler,
963 D. W., Schlesinger, W. H., and Tilman, D. G.: Human alteration of the global nitrogen
964 cycle: sources and consequences, Ecol. Appl., 7, 737-750, 1997.
965 Wesely, M., and Hicks, B.: Some factors that affect the deposition rates of sulfur
966 dioxide and similar gases on vegetation, Journal of the Air Pollution Control
967 Association, 27, 1110-1116, 1977.
968 Whitburn, S., Van Damme, M., Clarisse, L., Bauduin, S., Heald, C. L., Hadji-Lazaro,
969 J., Hurtmans, D., Zondlo, M. A., Clerbaux, C., and Coheur, P. F.: A flexible and robust
970 neural network IASI-$NH_3$ retrieval algorithm, J. Geophys. Res-Atmos., 121,
971 6581-6599, 10.1002/2016JD024828, 2016.
972 Williams, J. E., Boersma, K. F., Le Sager, P., and Verstraeten, W. W.: The
973 high-resolution version of TM5-MP for optimized satellite retrievals: description and
974 validation, Geosci. Model Dev., 10, 721-750, 10.5194/gmd-10-721-2017, 2017.
975 Wong, D. C., Pleim, J., Mathur, R., Binkowski, F., Otte, T., Gilliam, R., Pouliot, G.,
976 Xiu, A., Young, J. O., and Kang, D.: WRF-CMAQ two-way coupled system with
977 aerosol feedback: software development and preliminary results, Geosci. Model Dev.,

978 5, 299-312, 10.5194/gmd-5-299-2012, 2012.
979 Xu, W., Luo, X. S., Pan, Y. P., Zhang, L., Tang, A. H., Shen, J. L., Zhang, Y., Li, K. H.,
980 Wu, Q. H., Yang, D. W., Zhang, Y. Y., Xue, J., Li, W. Q., Li, Q. Q., Tang, L., Lv, S. H.,
981 Liang, T., Tong, Y. A., Liu, P., Zhang, Q., Xiong, Z. Q., Shi, X. J., Wu, L. H., Shi, W.
982 Q., Tian, K., Zhong, X. H., Shi, K., Tang, Q. Y., Zhang, L. J., Huang, J. L., He, C. E.,
983 Kuang, F. H., Zhu, B., Liu, H., Jin, X., Xin, Y. J., SHi, X. K., Du, E. Z., Dore, A. J.,
984 Tang, S., Collett Jr, J. L., Goulding, K., Sun, Y. X., Ren, J., Zhang, F. S., and Liu, X. J.:
985 Quantifying atmospheric nitrogen deposition through a nationwide monitoring
986 network across China, Atmos. Chem. Phys., 15, 12345-12360, 2015.
987 Yu, G., Jia, Y., He, N., Zhu, J., Chen, Z., Wang, Q., Piao, S., Liu, X., He, H., Guo, X.,
988 Wen, Z., Li, P., Ding, G., and Goulding, K.: Stabilization of atmospheric nitrogen
989 deposition in China over the past decade, Nat. Geosci., 12, 424-429,
990 10.1038/s41561-019-0352-4, 2019.
991 Zhang, L., Wright, L. P., and Asman, W. A. H.: Bi-directional air-surface exchange of
992 atmospheric ammonia: A review of measurements and a development of a big-leaf
993 model for applications in regional-scale air-quality models, J. Geophys. Res-Atmos.,
994 115, 898-907, 2010.
995 Zhang, L., Jacob, D. J., Knipping, E. M., Kumar, N., Munger, J. W., Carouge, C., Van
996 Donkelaar, A., Wang, Y., and Chen, D.: Nitrogen deposition to the United States:
997 distribution, sources, and processes, Atmos. Chem. Phys., 12 4539-4554, 2012.
998 Zhang, Q., Streets, D. G., Carmichael, G. R., He, K., Huo, H., Kannari, A., Klimont,
999 Z., Park, I., Reddy, S., and Fu, J.: Asian emissions in 2006 for the NASA INTEX-B

mission, Atmos. Chem. Phys., 9, 5131-5153, 2009.

Zhang, X. Y., Lu, X. H., Liu, L., Chen, D. M., Zhang, X. M., Liu, X. J., and Zhang, Y.: Dry deposition of $NO_2$ over China inferred from OMI columnar $NO_2$ and atmospheric chemistry transport model, Atmos. Environ., 169, 2017.

Zhang, X. Y., Chuai, X. W., Liu, L., Zhang, W. T., Lu, X. H., Zhao, L. M., and Chen, D. M.: Decadal Trends in Wet Sulfur Deposition in China Estimated From OMI $SO_2$ Columns, J. Geophys. Res-Atmos., 123, 10796-10811, 10.1029/2018JD028770, 2018.

Zhao, X., Chen, L., and Zhang, H.: Nitrate and ammonia contaminations in drinking water and the affecting factors in Hailun, northeast China, Journal of Environmental Health, 75, 28, 2013.

Zhao, Y., Zhang, L., Chen, Y., Liu, X., Xu, W., Pan, Y., and Duan, L.: Atmospheric nitrogen deposition to China: A model analysis on nitrogen budget and critical load exceedance, Atmos. Environ., 153, 32-40, http://dx.doi.org/10.1016/j.atmosenv.2017.01.018, 2017.